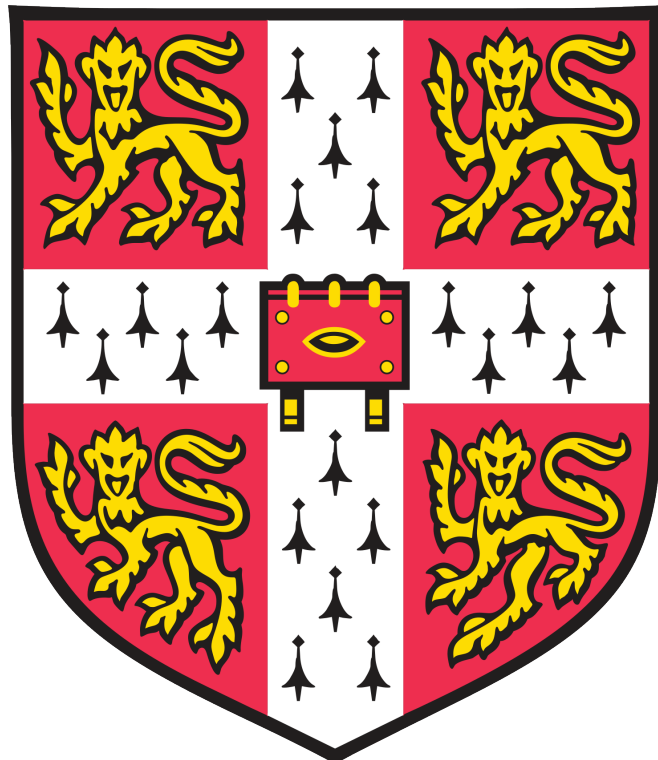


**Joshua Bird**

# **Distributed Visual Simultaneous Localization and Mapping**



Computer Science Tripos – Part II  
Queens' College

May 10, 2024

## **Declaration**

I, Joshua Bird of Queens' College, being a candidate for Part II of the Computer Science Tripos, hereby declare that this dissertation and the work described in it are my own work, unaided except as may be specified below, and that the dissertation does not contain material that has already been used to any substantial extent for a comparable purpose. In preparation of this dissertation I did not use text from AI-assisted platforms generating natural language answers to user queries, including but not limited to ChatGPT. I am content for my dissertation to be made available to the students and staff of the University.

*Signed:* Joshua Bird

*Date:* May 10, 2024

# Proforma

Candidate number: 2377E  
Project Title: **Distributed Visual Simultaneous Localization and Mapping**  
Examination: **Computer Science Tripos – Part II, 2024**  
Word Count: 11966<sup>1</sup>  
Code Line Count: 35,250<sup>2</sup> (8,194 modified<sup>3</sup>)  
Project Originator: The candidate and Jan Blumenkamp  
Project Supervisor: Jan Blumenkamp

## Original Aims of the Project

This project aimed to develop a distributed visual simultaneous localization and mapping system that enables multiple agents to localize themselves within a collaboratively built map of the world using purely visual data. Additionally, agents should be able to act independently, failing gracefully if communication with their peers is lost. This would be followed by a quantitative evaluation of my system when run on industry-standard datasets.

## Work Completed

All success criteria have been met, with significant additional work being conducted. My system implements a novel approach to distributed visual simultaneous localization and mapping, outperforming comparable state-of-the-art systems on standard datasets. In addition, my system has been deployed on physical robots to demonstrate its real-world performance. Finally, considerable work has been put into developing generic infrastructure for my project including evaluation, simulation, and visualization tools, all of which have been made open-source alongside my core project. My work has been included in the paper *The Cambridge RoboMaster: An Agile Multi-Robot Research Platform*, of which I am an author.

## Special Difficulties

None.

---

<sup>1</sup>This word count was computed using `texcount`.

<sup>2</sup>This code line count was computed using `cloc`, and excludes third party libraries and configuration files.

<sup>3</sup>As my dissertation includes external code, I have calculated the number of lines of code explicitly modified by myself using `git diff`. This excludes mass file deletion and formatting.

# Contents

<b>1</b>	<b>Introduction</b>	<b>1</b>
1.1	Motivation . . . . .	1
1.2	Project Overview . . . . .	2
<b>2</b>	<b>Preparation</b>	<b>3</b>
2.1	Starting Point . . . . .	3
2.2	Visual SLAM Background . . . . .	3
2.2.1	Visual Odometry . . . . .	3
2.2.2	Towards Visual SLAM . . . . .	4
2.2.3	Tracking . . . . .	5
2.2.4	Mapping . . . . .	5
2.2.5	Loop Closure . . . . .	5
2.3	Relevant Work . . . . .	6
2.4	Algorithms . . . . .	7
2.4.1	Kabsch-Umeyama Algorithm . . . . .	7
2.4.2	RANSAC . . . . .	8
2.4.3	Visual Bag of Words . . . . .	8
2.5	Requirements Analysis . . . . .	9
2.5.1	Development Model . . . . .	9
2.6	Development Tools & Frameworks . . . . .	10
2.6.1	Webots Simulation Software . . . . .	10
2.6.2	Testing Infrastructure . . . . .	11
2.6.3	Robot Operating System 2 Communication Middleware . . . . .	11
2.6.4	Docker and Continuous Integration / Continuous Deployment . . . . .	11
2.7	Datasets . . . . .	12
2.8	Licensing . . . . .	12
<b>3</b>	<b>Implementation</b>	<b>13</b>
3.1	Agent Architectural Overview . . . . .	13
3.2	SLAM System . . . . .	14
3.2.1	Data Structures . . . . .	14
3.2.2	Decentralized System Manager . . . . .	15
3.2.3	State Manager . . . . .	15
3.2.4	Map Serialization and Deserialization . . . . .	15
3.2.5	External Map Merge Finder . . . . .	16
3.2.6	External Map Merger . . . . .	17
3.2.7	External KeyFrame Inserter . . . . .	19

3.2.8	Local KeyFrame Inserter . . . . .	20
3.2.9	Generalizing to $N \geq 3$ Agent Systems . . . . .	21
3.2.10	Map Alignment Refiner . . . . .	22
3.2.11	Losing Localization / Connection . . . . .	23
3.2.12	Visualization Publisher . . . . .	24
3.3	Motion Controller . . . . .	24
3.3.1	Follow The Leader . . . . .	24
3.3.2	Multi-Agent Collision Avoidance . . . . .	24
3.3.2.1	Non-Linear Model Predictive Controller Formulation . . . . .	24
3.3.2.2	Implementation Details . . . . .	25
3.4	Central Management Interface . . . . .	26
3.5	Custom Evaluation Suite – Multi-Agent EVO . . . . .	27
3.6	Simulation Environment . . . . .	28
3.7	Real World Implementation . . . . .	28
3.7.1	Cambridge RoboMaster Platform . . . . .	29
3.7.2	OptiTrack Motion Capture System . . . . .	29
3.7.3	Raspberry Pi Video Publisher . . . . .	29
3.7.4	Augmented Reality Visualization . . . . .	30
3.8	Repository Overview . . . . .	31
<b>4</b>	<b>Evaluation</b>	<b>33</b>
4.1	Review of Success Criteria . . . . .	33
4.2	Benchmarking . . . . .	33
4.2.1	EuRoC Machine Hall . . . . .	34
4.2.2	TUM-VI Rooms . . . . .	35
4.3	Comparison to Related Work . . . . .	36
4.3.1	CCM-SLAM . . . . .	37
4.3.2	VINS-Mono Multisession SLAM . . . . .	37
4.3.3	Comparison to Single-Agent SLAM Systems . . . . .	38
4.4	Real World Experiments . . . . .	38
4.4.1	Multi-Agent Collision Avoidance . . . . .	39
<b>5</b>	<b>Conclusions</b>	<b>40</b>
5.1	Future Work . . . . .	40
5.2	Lessons Learned . . . . .	40
<b>Bibliography</b>		<b>41</b>
<b>A Additional Figures</b>		<b>44</b>
<b>B Project Proposal</b>		<b>45</b>

# Chapter 1

## Introduction

Visual Simultaneous Localization and Mapping (visual SLAM) serves as the foundation of countless modern technologies, with self-driving cars, augmented reality devices, and autonomous drones just being a few examples. By using purely visual inputs, visual SLAM is able to create a 3D map of the surroundings while also localizing the camera's position within this map in real-time.

Unlike other SLAM systems which may use expensive and heavy sensors such as LIDAR, RGB-Depth cameras, or Radar, visual SLAM only requires the ubiquitous camera sensor, allowing the technology to be used in many commercial applications such as Google's ARCore [1], Boston Dynamic's GraphNav system used on their robot Spot [2], and several models of DJI quadcopters [3], underscoring the practicality of this research field.

### 1.1 Motivation

Multi-robot systems are becoming increasingly common as automation continues to grow across a variety of sectors, including self-driving cars, drone swarms, and warehouse robots. These systems require the agents to understand the world around them as well as their peers' locations within that world. This task is typically achieved through technologies such as GPS or motion capture setups, however, not all environments have access to these systems. A few emerging examples include:

- Search and rescue operations in large indoor environments, assisted by drone swarms.
- Self-driving cars in underground road networks.
- Multi-agent extraterrestrial exploration.

These are scenarios where multi-agent SLAM provides a compelling solution, it allows for mapping unfamiliar environments while maintaining awareness of the positions of all agents involved. However, many of the existing multi-agent visual SLAM implementations are centralized systems, requiring agents to maintain a reliable communication link with a central server in order to operate. This is severely disadvantageous, as environments lacking access to GPS or motion capture systems often also suffer from unreliable communication channels – greatly limiting the use cases of these centralized multi-agent SLAM systems.

Naturally, this leaves us with distributed multi-agent visual SLAM systems that do not rely on a central management server, allowing the agents to be deployed in environments where network infrastructure may be lacking. Instead of utilizing a central node, the agents communicate peer-to-peer when they come within close proximity to one another.

It is easy to see the broad-reaching use cases of such a system. Agents will be able to explore sections of their world independently, or in small teams, sharing new world locations with their peers as they come into communication range using an ad-hoc network. Additionally, agents will be able to accurately determine their peers' locations when they are within communication range, allowing for collision avoidance and cooperative path planning.

## 1.2 Project Overview

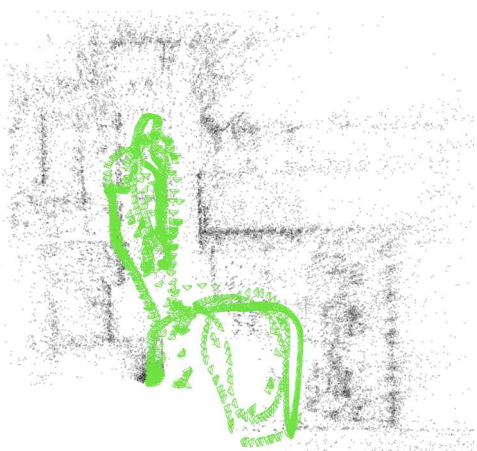
In this project, I:

1. Design and implement a novel distributed monocular visual SLAM system, capable of localization, relative pose estimation, and collaborative mapping, all while being tolerant to degraded network conditions and not reliant on any single leader agent (section 3.2).
2. Evaluate the performance of my system on standard datasets, **demonstrating its superior performance over comparable state-of-the-art systems** (section 4.3).
3. Create a simulation environment for testing and evaluating my system locally (section 3.6).
4. Develop a custom collision avoidance framework (section 3.3) and deploy it alongside my SLAM system on physical robots, **demonstrating the practical use cases of my system and benchmarking real-world performance** (section 4.4).
5. **Contribute as a co-author to the paper *The Cambridge RoboMaster: An Agile Multi-Robot Research Platform* [4].** My distributed SLAM system is included in the paper and used to evaluate the robotics platform (section 3.7.1).
6. Develop *Multi-Agent EVO* – the first open-source evaluation library for multi-agent SLAM systems (section 3.5).
7. Develop the *Raspberry Pi Video Publisher* – a performant platform for SLAM data collection and augmented reality visualizations – and set up a continuous integration and deployment pipeline to automatically deploy the latest builds to the devices (section 3.7.3).

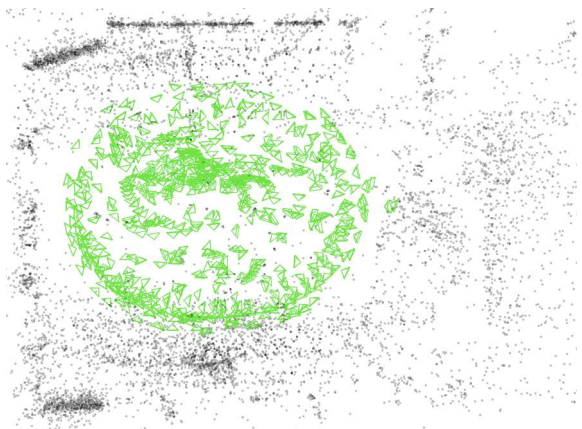
A short video demonstration of my project is provided at the following URL:

<https://cam-diss.s3.amazonaws.com/video.mp4>

Due to the highly visual and 3D nature of my project, **I strongly recommend viewing the video.** It will provide an intuition of my system, making the following chapters easier to visualize and understand. Additionally, it is referenced throughout this dissertation.



(a) EuRoC Machine Hall 01-03



(b) TUM-VI Rooms 1-3

The figures above display the maps collaboratively built by my distributed SLAM system using only monocular videos from industry-standard multi-agent datasets.

# Chapter 2

## Preparation

### 2.1 Starting Point

Visual SLAM systems are a mature and well-researched field of computer science, with many advanced existing implementations. To avoid spending the majority of my effort re-implementing a visual SLAM system from scratch, I chose to use a **single-agent** visual SLAM implementation as the starting point for my project. The rationale behind this decision was that it would allow me to focus my efforts on the distributed multi-agent aspect of this project, which I believe is the novel and under-researched aspect of the field.

I chose ORB-SLAM3 [5] as the single-agent SLAM system to base my system on top of, as it ranks at the top of benchmarks in a variety of environments [6] and its codebase is publically available. I primarily utilized the system's **tracking** and **local mapping** modules, as well as some helper functions from the backend, which are all attributed during the discussion of my algorithms in the Implementation section.

While ORB-SLAM3 is an excellent SLAM system, it is fundamentally a single-agent system with no considerations in place for use in a multi-agent context. As I will later expand upon, a significant amount of time and effort was required to understand its extremely large and undocumented codebase, especially since an almost complete understanding of its inner workings was needed to both extract and inject map information from the system. In retrospect, basing my project on an existing single-agent SLAM system did not save as much time as I had hoped, as it took almost a month to get ORB-SLAM compiled and running locally, and many more before I was able to make good progress on the distributed aspect of my project.

At the time of submitting my project proposal, I had forked the ORB-SLAM3 git repository<sup>1</sup> and explored the codebase. I had no prior experience with SLAM systems but did research the current state of multi-agent visual SLAM to evaluate the feasibility of my project and to prevent it from being a duplication of prior work.

### 2.2 Visual SLAM Background

Before developing a distributed multi-agent SLAM system, we must first understand the basics of a visual SLAM. This is a topic on which numerous books [7] [8] and research papers [9] [10] [11] have discussed in depth, which I will attempt to summarize below.

#### 2.2.1 Visual Odometry

To grasp visual SLAM effectively, it is useful to start with a foundational concept – visual odometry (VO). VO is the process of estimating the trajectory of a camera based on the sequence of images produced by it. The core idea is to track features across consecutive images, observing how the features move relative to one another to infer the motion of the camera.

Take, for example, the two images from the KITTI00 dataset [12] presented in Figure 2.1. We can see that Figure 2.1b is taken a few meters in front of Figure 2.1a.

---

<sup>1</sup>[https://github.com/UZ-SLAMLab/ORB\\_SLAM3](https://github.com/UZ-SLAMLab/ORB_SLAM3)



(a)



(b)

**Figure 2.1:** Example images from KITTI00 dataset for the visual odometry example.

The first step towards determining the change in pose is identifying common features in both images. For this, we use feature descriptors, which find recognizable details within the image and represent them as vectors. The ORB descriptor [13] is frequently used in VO and SLAM due to its low computational cost and invariance to rotation and scale, making it our choice for this example.

Figure 2.2 displays the ORB feature matches between the two images, however it is clear that many of them are incorrect. This is to be expected, as many elements of the images are repeated such as the windows and tree branches.



**Figure 2.2:** Feature descriptor matches between the two images.

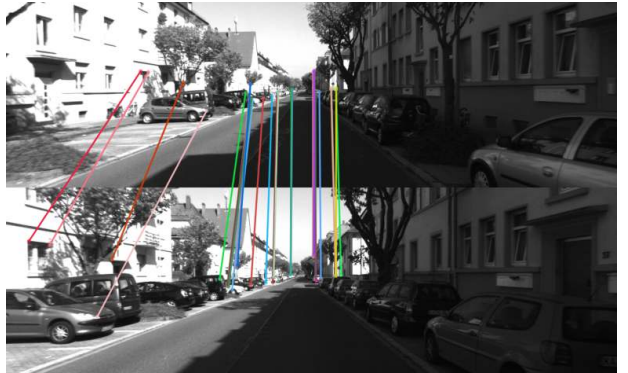


**Figure 2.3:** Inlier feature descriptors after fitting the data to the epipolar geometry model using RANSAC.

We can remove the majority of incorrect correlations by constraining the matches to the epipolar geometry model [14] – essentially telling the algorithm that the two images are the same scene captured from two different camera poses. Since there are a lot of outliers we use the RANSAC algorithm, later defined in section 2.4.2, to fit the data to this epipolar geometry model. This results in the subset of matches shown in Figure 2.3, which are far more accurate.

We can now run the seven-point algorithm [14] on the matches to extract the rotation  $\mathbf{R}$  and translation  $\mathbf{t}$  between the two images, and consequently triangulate the world features found in both images. This is displayed in Figure 2.4. By continuing this process for all image pairs in a video, we can estimate the trajectory of the camera as it moves through the world. It is important to note that the scale of the world is arbitrary when only using monocular video.

## 2.2.2 Towards Visual SLAM

Visual odometry provides a local estimate of trajectories, however, it does not build a map of the world and therefore can not give an accurate global estimate of the agent’s trajectory. Visual SLAM addresses this problem by mapping the environment as it moves through it, using this map to localize itself within the world. Modern systems typically break this down into three processes: Tracking, Mapping, and Loop Closing.

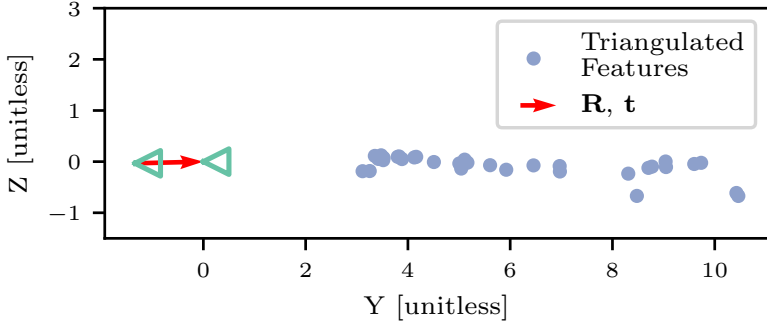


**Figure 2.4:** Side view of the estimated  $\mathbf{R}$  and  $\mathbf{t}$  between the two camera poses, and the triangulated feature points.

### 2.2.3 Tracking

The tracking step processes image data to compute the pose of the agent within the map. This step leverages many of the core ideas from visual odometry, using feature descriptors to find matches and fitting them to the epipolar geometry model using RANSAC. However, instead of matching features between consecutive images like visual odometry, we find feature matches between the input image and the 3D map of feature points we have built.

### 2.2.4 Mapping

Mapping extracts the data gathered during the tracking phase to create a 3D representation of the environment. Many popular visual SLAM implementations use a keyframe-based approach, where the map is estimated using only a few select image frames, ignoring the intermediate frames which provide little additional information. This effectively decouples the mapping and tracking processes, allowing us to perform relatively costly but very effective pose graph optimizations.

**Pose Graph Optimization (PGO)** is the process of minimizing the errors within our map, typically through the use of a graph optimizer. We represent keyframes and world features as nodes in our graph, with edges representing the constraints between nodes through an attached cost function. For example, if a keyframe observes a feature at position  $(-0.23, 0.64)$  in their image, an edge between the keyframe and feature will be created with a cost function that is minimized when our map reprojects the feature onto the keyframe at the observed point. Similar edge constraints can be defined between keyframes using IMU measurements or wheel odometry.

We can intuitively think of the edge constraints as springs (Figure 2.5), all attempting to revert to their preferred length (given by the world observations). The graph optimizer moves the keyframes and features around until the system settles into its lowest energy state, where the map agrees with our observations as closely as possible.

### 2.2.5 Loop Closure

Loop closing is crucial for maintaining the long-term accuracy of the SLAM system. It involves recognizing when the agent re-visits a previously mapped location and “closes the loop” by correcting the errors that have accumulated over time. We often vectorize keyframes’ images using the visual bag of words approach (later explained in section 2.4.3) to identify when an agent re-visits an area. When a loop closure is detected, we fuse the duplicate features and use pose graph optimization to re-optimize the map and ensure global consistency, as illustrated in Figure 2.6.

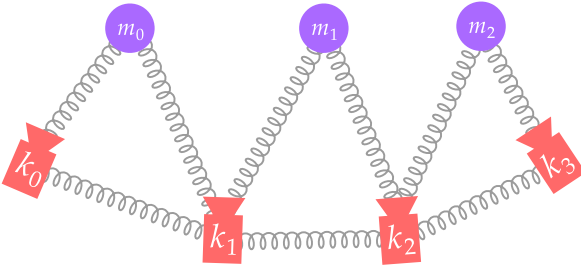
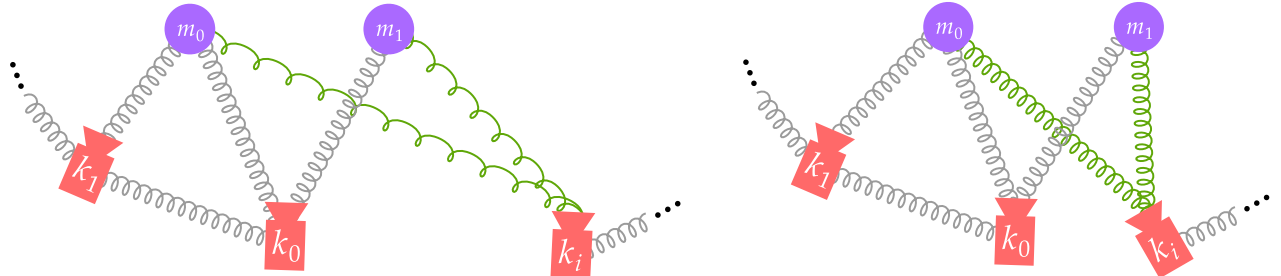


**Figure 2.5:** Graph pose optimization diagram, where  $k_i$  is a keyframe and  $m_i$  is a feature point. The springs represent constraints between the nodes.



(a) A loop closure is identified and new constraints are added between  $k_i$  and  $m_0, m_1$ . The new constraints are initially “stretched” since  $m_0$  and  $m_1$ ’s location in the map does not correlate with  $k_i$ ’s observation of them.

(b) The graph optimizer adjusts the keyframes and feature point poses so the map better aligns with the observations.

**Figure 2.6:** Loop closure pose graph optimization. The green edges represent the new constraints added by the loop closure.

## 2.3 Relevant Work

While single-agent SLAM systems are a relatively mature field of research, multi-agent systems are still very much in active development.

Centralized multi-agent systems such as CCM-SLAM [15] and COVINS [16] require a centralized server to perform map merges and PGO. While simpler to implement, this comes with the obvious limitations of centralized systems such as scalability and robustness issues, as well as requiring existing networking infrastructure.

In recent years we have seen the emergence of a handful of decentralized multi-agent systems, however, many of them have various limitations. Systems such as [17] [18] [19] require the agents to be initialized with their ground truth poses, which greatly limits their real-world usability. In contrast, my system is able to provide accurate relative localization even when agents are initialized in arbitrary and unknown locations by identifying common landmarks in the world.

Figure 2.7 lays out the sensor configurations used by popular state-of-the-art multi-agent SLAM systems, showing that my system is one of the only distributed systems capable of operating with purely monocular visual data<sup>1</sup>. This is advantageous, as LiDAR & RGBD sensors have considerable weight, and stereo cameras may require a minimum camera separation to operate,

<sup>1</sup>There are several other monocular-only systems published in the field [20] [21] [22]. However, unlike the other systems discussed in this dissertation, they have not made their source code available, nor have they reported their system’s performance on publicly accessible datasets. Unfortunately, this makes any meaningful comparison to their systems impossible.

both of which limit their usability on devices such as small aerial robots. However, using only monocular video introduces several challenges, such as less data being available to perform tracking and mapping, and arbitrary map scale.

System	Year	Collaboration Type	Monocular	Stereo	Monocular +IMU	Stereo +IMU	LiDAR +IMU	RGBD +IMU
<b>My System</b>	2024	Decentralized	X					
<i>D<sup>2</sup>SLAM [23]</i>	2022	Decentralized				X		
<b>CCM-SLAM [15]</b>	2019	Centralized	X					
<b>COVINS [16]</b>	2021	Centralized			X			
<b>Kimera-multi [24]</b>	2021	Decentralized				X		X
<b>Swarm-SLAM [25]</b>	2024	Decentralized				X	X	X
<b>DOOR-SLAM [26]</b>	2020	Decentralized				X		

**Figure 2.7:** Comparison of popular multi-agent SLAM systems. My SLAM system stands out as one of the only modern decentralized monocular systems available.

Additionally, my system provides a novel approach to the Distributed Pose Graph Optimization (DPGO) problem<sup>1</sup>. There are various approaches to DPGO. SWARM-SLAM [27] elects a single agent to perform the PGO for the entire swarm, which is simple but has a high communication overhead since all agents have to send their pose estimations before each optimization. Other systems perform DPGO by spreading computation across agents through the use of distributed optimization frameworks such as ARock [28] or Distributed Gauss-Seidel [29], however, these methods still present a communication overhead and may stall in when presented with unreliable communications.

Instead of performing discrete optimization runs, my method of DPGO is performed incrementally. Each agent optimizes its pose graph as external data streams in, with a separate map alignment step. This method has no additional communication overhead, apart from the infrequent map alignment step, however, it comes at the cost of less verifiable global consistency. We evaluate my method’s performance in the Benchmarking section, demonstrating its very competitive real-world performance. The details of my implementation are presented in the Decentralized System Manager section.

## 2.4 Algorithms

### 2.4.1 Kabsch-Umeyama Algorithm

The Kabsch-Umeyama algorithm (Algorithm 1) is used to align a set of target points  $Q$  to a set of source points  $P$  through a  $\text{SIM}(3)$  transformation<sup>2</sup>. Within the field of SLAM, this is commonly used to align estimated trajectories with the ground truth, as it may be translated, rotated, and scaled differently to the ground truth. Additionally, this algorithm is used in my multi-agent map alignment process.

<sup>1</sup>Distributed pose graph optimization is the multi-agent extension of the pose graph optimization problem introduced in section 2.2.4.

<sup>2</sup>A  $\text{SIM}(3)$  transform is the composition of a translation, rotation, and uniform scale in three-dimensional space.

---

**Algorithm 1** Kabsch-Umeyama Algorithm

---

```
1: Input: Source points  $P$ , target points  $Q$ 
2: Output: Rotation  $R$ , scale  $s$ , and translation  $t$  that best aligns  $Q$  to  $P$ 
3:  $n \leftarrow$  number of points in each set
4:  $\mu_P \leftarrow \frac{1}{n} \sum_{i=1}^n p_i$ 
5:  $\mu_Q \leftarrow \frac{1}{n} \sum_{i=1}^n q_i$ 
6:  $P' \leftarrow P - \mu_P$                                  $\triangleright$  Centering  $P$ 
7:  $Q' \leftarrow Q - \mu_Q$                                  $\triangleright$  Centering  $Q$ 
8:  $\sigma_P^2 \leftarrow \frac{1}{n} \sum_{i=1}^n \|p'_i\|^2$        $\triangleright$  Variance of  $P$ 
9:  $H \leftarrow \frac{1}{n} \sum_{i=1}^n p_i'^T q_i'$            $\triangleright$  Covariance matrix
10:  $U, D, V^T \leftarrow \text{SVD}(H)$                    $\triangleright$  Singular Value Decomposition
11:  $S \leftarrow \text{diag}(1, 1, \dots, 1, \det(U) \det(V^T))$ 
12:  $R \leftarrow USV^T$                                  $\triangleright$  Rotation matrix
13:  $c \leftarrow \frac{\sigma_P^2}{\text{tr}(DS)}$              $\triangleright$  Scale factor
14:  $t \leftarrow \mu_P - cR\mu_Q$                        $\triangleright$  Translation
15: return  $R, s, t$ 
```

---

## 2.4.2 RANSAC

RANDOM SAmple Consensus (RANSAC) is an iterative method used to robustly fit a mathematical model to a dataset with a large number of outliers, without the outliers having any influence over the estimated model. This is particularly useful in visual SLAM as observations are extremely noisy, often containing far more outliers than inliers. Pseudocode for the algorithm is presented in Algorithm 2.

---

**Algorithm 2** RANSAC Algorithm

---

```
1: Input: datapoints, model to explain data, number of iterations  $k$ , threshold  $\tau$ , minimum
   number of data points needed to fit model  $n$ 
2: Output: Best fitting model
3:  $\text{bestModel} \leftarrow \text{null}$ 
4:  $\text{bestInliers} \leftarrow \{\}$ 
5: for  $i = 1$  to  $k$  do
6:    $\text{samples} \leftarrow n$  randomly selected data points
7:    $\text{model} \leftarrow \text{model fit to samples}$ 
8:    $\text{inliers} \leftarrow \{\}$ 
9:   for each point in datapoints do
10:    if point fits model with error  $< \tau$  then
11:      Add point to inliers
12:    if number of inliers  $>$  size of bestInliers then
13:       $\text{bestInliers} \leftarrow \text{inliers}$ 
14:       $\text{bestModel} \leftarrow \text{model}$ 
15: return bestModel
```

---

## 2.4.3 Visual Bag of Words

The visual bag of words algorithm is used to vectorize an image based on its features, allowing us to compare how similar two images are. My system utilizes this to efficiently detect potential map merges between agents.

To convert our image to a vector, we must first build a *vocabulary* of features: common and unique features that will each go on to represent a dimension of our image vector. We do this by extracting features from a large dataset of images and grouping their descriptors using an algorithm such as K-Means clustering. The centers of the clusters can then be used as our feature vocabulary. A visual overview of the process is given in Figure 2.8. This vocabulary generation step only needs to be performed once, preferably using a wide variety of representative images (for visual SLAM, this should be images from a variety of environments).

We are now able to vectorize images by counting the number of times each feature within our vocabulary exists in the image (Figure 2.9).

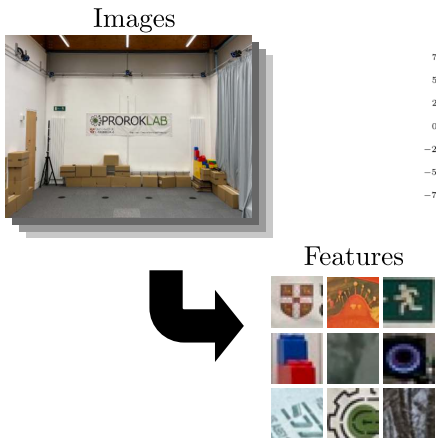


**Figure 2.8:** Process of generating the visual bag of word vocabulary. The center of each cluster is added as a feature in the vocabulary and will represent a distinct vector dimension.

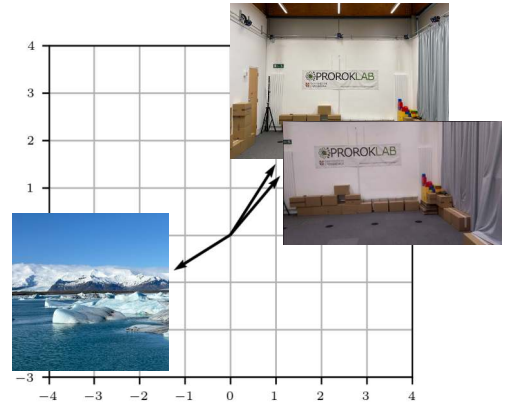


**Figure 2.9:** Visualization of image vectorization using the visual bag of words method. Images sharing common features result in closely aligned vectors.

## 2.5 Requirements Analysis

After further background reading of the relevant literature and a review of other multi-agent SLAM systems, I broke my project down into the requirements shown in Figure 2.10. Features vital to achieving my core deliverables are given high importance, while extensions are given low importance. Additionally, features are given a risk level to help with planning and time allocation.

### 2.5.1 Development Model

This project best lends itself to the Spiral Development Model [30], as it consists of multiple well-defined features but requires frequent review and planning to decide what direction to push the project forward next. Developing my SLAM system was a large software engineering undertaking, involving the development of 5 ROS packages, an evaluation library, and even hardware. I knew that a rigid plan would quickly fall apart as roadblocks occurred, and therefore, I chose the spiral model as it allowed me to adapt my plan as risks were identified and priorities changed.

After implementing each core feature of my SLAM system, I would evaluate its performance with my testing and evaluation infrastructure to identify any unexpected issues and identify potential risks. This would influence my plan for the next iteration around the spiral, as well as my long-term plan for the project.

Feature	Importance	Risk
Simulation environment	High	Low
ORB-SLAM3 integration	High	Medium
Map serialization/deserialization	High	Medium
Decentralized system state manager	High	Low
Map merge finder and merger	High	Low
Handle losing communication	High	Low
Management interface	Medium	Low
Distributed pose graph optimization	Low	High
Map compression	Low	Medium
Visualization tools	Low	Low
Additional sensors	Low	High
Intelligent map sharing	Low	Medium
Motion controller <sup>1</sup>	Low	Medium
Real-world deployment <sup>1</sup>	Low	Medium
Augmented Reality visualization <sup>1</sup>	Low	High

**Figure 2.10:** Risk analysis. <sup>1</sup>Requirement added after work had begun.

A good example of a pivot taken after re-evaluating my project was in late January, when the core features of my project were complete and I was planning the next stage of development. Discussions with my supervisor, as well as my own analysis of the project, revealed that the original extensions were no longer very relevant to my project, as they either had implicitly been achieved while developing my core features or would not yield particularly interesting results. We instead decided to focus on deploying to real robots to demonstrate real-world usability and performance. I am glad that I made this choice, as I believe it greatly strengthens the credibility of my SLAM system.

## 2.6 Development Tools & Frameworks

Due to the scale of this software engineering project, I knew that a well-structured development plan and carefully chosen frameworks would be essential to its successful implementation. Much thought was put into using frameworks such as ROS and Docker, which led to smooth development and allowed my system to easily be deployed to real-world robots.

In addition, an entire suite of infrastructure was created to aid the development of my distributed SLAM system, including simulation environments, an evaluation library, visualization tools, and testing infrastructure.

### 2.6.1 Webots Simulation Software

Robotics projects work in the physical domain, however testing in the real world requires a large amount of setup and infrastructure. To ensure fast iteration, I decided to use simulations for the majority of my development. This allowed me to easily test my system in various environments and scenarios before deploying it to physical robots.

I chose to use the open-source robotics simulator Webots [31], due to its well-documented API and realistic renders. The details of integrating Webots into my project are explored in section 3.6, including the ROS interfaces developed and agent controllers.

## 2.6.2 Testing Infrastructure

Along with being very useful for real-time testing, the simulation software enabled me to record numerous test cases which I have used as regression tests and benchmarks for my system throughout development. There are datasets for testing all core functionality of my SLAM system, which I would run at regular intervals during development to ensure that no features had regressed and to ensure performance was improving.

## 2.6.3 Robot Operating System 2 Communication Middleware

Robot Operating System (ROS) 2 is the glue holding my system together, allowing independent software processes and hardware to communicate through a standardized messaging interface.

ROS has long been the industry standard, being almost ubiquitous in both robotics research and the commercial sector. Confusingly, ROS is not an operating system at all, but instead, a cross-platform development framework that provides a middleware to facilitate reliable communication between independent processes called *nodes*. These nodes can be on the same device or a device within the local area network and may be written in C++ or Python. Nodes communicate by *publishing* and *subscribing* to different *topics*, allowing both peer-to-peer and broadcast communication. Numerous custom *message types* had to be defined to specify the structure of messages sent between nodes.

Since every node is abstracted away behind the messaging interface, we can easily swap out nodes in this system. For example, we can substitute the real camera for a simulated camera to test my system in a virtual environment without having to change any other part of the system – as shown in Figure 2.11. This makes transitioning between the real and simulated world almost seamless, which I knew would be essential for the eventual deployment on to physical robots.

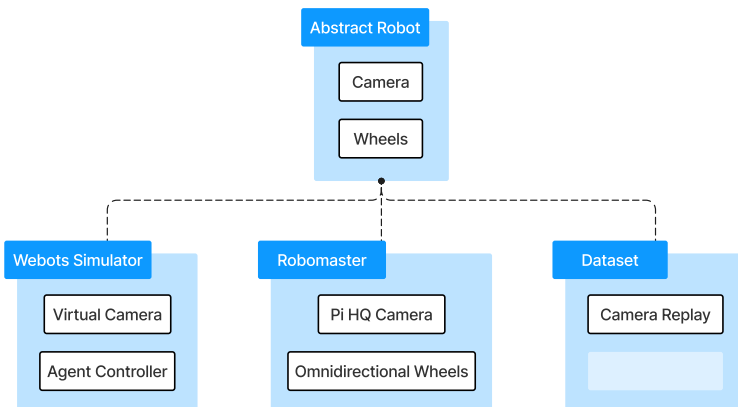


**Figure 2.11:** All robot types inherit the abstract robot interface as they all communicate over the same ROS message types. This allows my SLAM system and its supporting infrastructure to be completely agnostic to the actual type of robot used.

Furthermore, using the ROS framework allows my code to be portable, as anyone can download my nodes, link the camera topics up to their robot's camera, and run my SLAM system with minimal effort.

## 2.6.4 Docker and Continuous Integration / Continuous Deployment

My GitHub repositories are set up to perform continuous integration via GitHub Actions. Every time code is pushed to the repository, all 5 core packages (`central_management_interface`,

`interfaces, motion_controller, slam_system, webots_sim`) are built to ensure there are no compile time errors.

Additionally, a Docker container is cross-compiled to `arm64` and uploaded to Docker Hub. These Docker images can then be pulled to the Cambridge RoboMasters (introduced in section 3.7.1) and immediately run (Figure 2.12). This greatly speeds up development, as compiling the codebase locally on the Cambridge RoboMasters takes over 20 minutes for each robot.

Aside from the core packages, we also perform continuous integration as well as continuous deployment for the Raspberry Pi video publisher system (introduced in section 3.7.3). A Docker container is similarly cross-compiled to `arm64` and uploaded to Docker Hub, and it is automatically deployed to the Raspberry Pis so they will run the latest version of the package. Continuous deployment makes sense for this use case as the Raspberry Pis are designed to be plug-and-play, starting video streaming as soon as they are turned on, and we want them to use the latest software as soon as it is pushed to the GitHub repository.

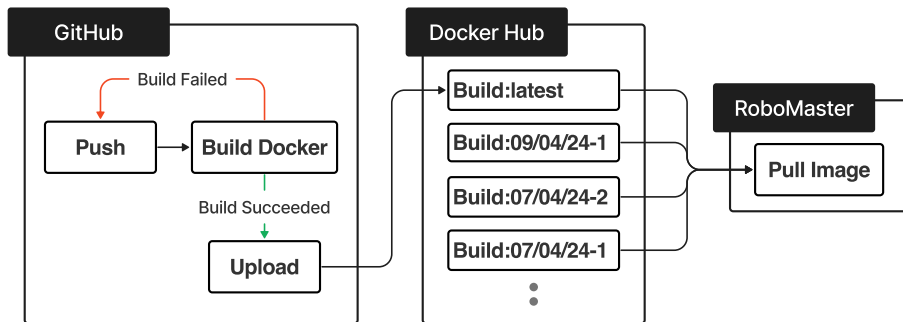


**Figure 2.12:** Automated continuous integration pipeline for the Cambridge RoboMasters. Continuous deployment is implemented for the Raspberry Pi video publishers by pulling from Docker Hub and running the container on startup.

Publishing my Docker containers on DockerHub not only simplifies development but also facilitates the easy deployment and evaluation of my system by third-party users. This approach aligns with the recommendations of Sharafutdinov et al. to avoid contributing to the reproducibility crisis that the field of SLAM research is currently facing [6].

## 2.7 Datasets

A variety of industry-standard datasets were utilized to benchmark the performance of my SLAM system, including the EuRoC Machine Hall [32] and TUM-VI [33] datasets. Further information about each dataset is provided in the Benchmarking section.

In addition to standard datasets, I also used the aforementioned custom datasets generated in the simulated environment for testing.

## 2.8 Licensing

All code is available as open-source software on GitHub. The core SLAM system and Multi-Agent EVO library are released under the GPL-3 license [34] as it builds upon code released under that license. My Raspberry Pi Video Publisher is published under the MIT license [35].

# Chapter 3

## Implementation

My project presents a novel approach to distributed visual SLAM which yields lower errors than comparable state-of-the-art systems. This improvement is a result of my system's extended capabilities, such as the ability for agents to recover from prolonged losses of localization, a unique approach to the distributed pose graph optimization problem, and algorithms that improve long-term map association & reuse. We also discuss the real-world deployment of my system and the necessary supporting infrastructure.

In addition, I introduce *Multi-Agent EVO* which, to my knowledge, is the first open-source multi-agent focused SLAM evaluation library, along with numerous other visualization, simulation, and control tools.

### 3.1 Agent Architectural Overview

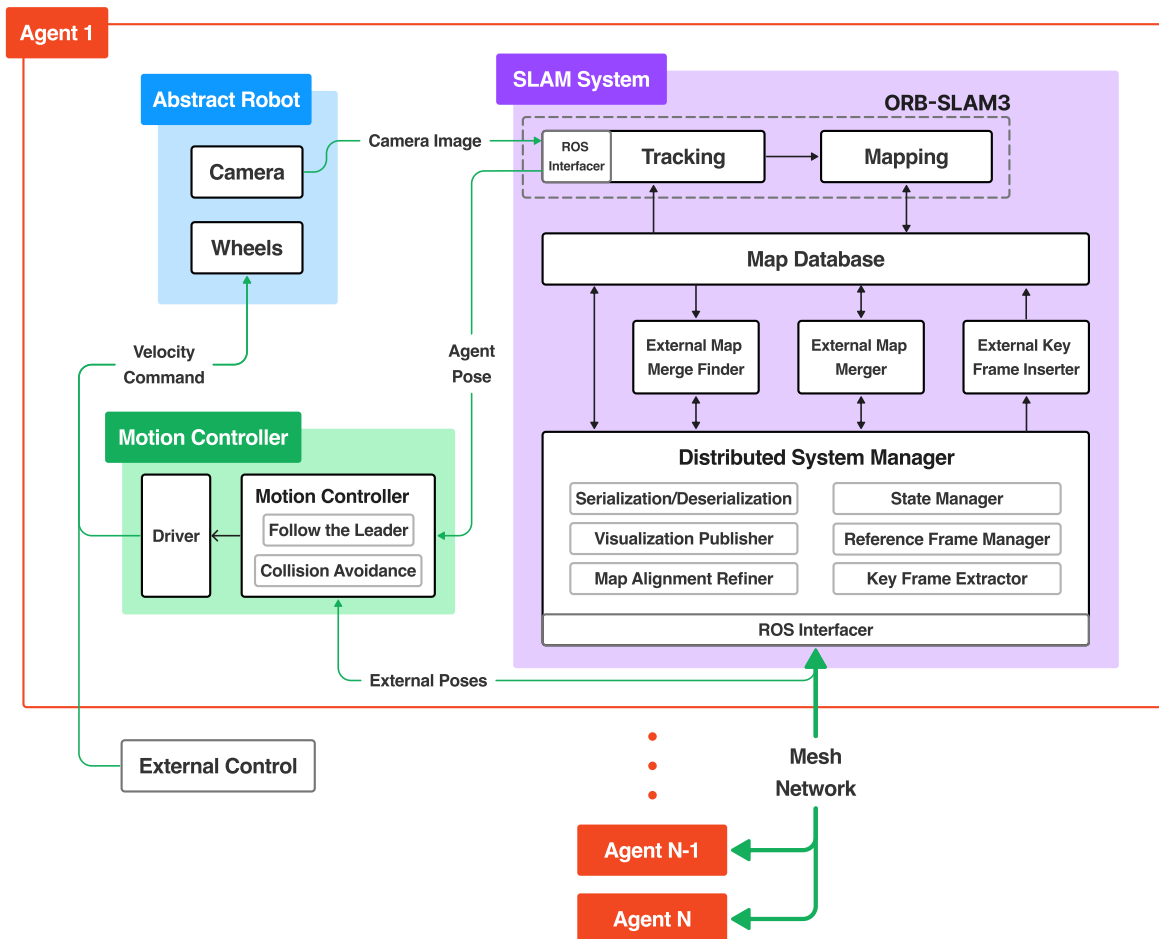


**Figure 3.1:** Agent diagram. Green arrows represent messages sent over ROS topics, while black arrows represent internal communications within a node.

Figure 3.1 gives an architectural overview of an agent in my system, showing how the **Abstract Robot**, **SLAM System** and **Motion Controller** ROS nodes interconnect.

From a high level, we have an **Abstract Robot** node that provides an interface to the robot's hardware. This sends camera images to the **SLAM System** node, which builds a map of the world in collaboration with its peers. The **Motion Controller** node receives agent pose information from both the local **SLAM System** and the external peers to perform tasks such as collision avoidance by sending velocity commands back to the **Abstract Robot** node, closing the control loop.

In the following sections, we will explore these nodes in detail.

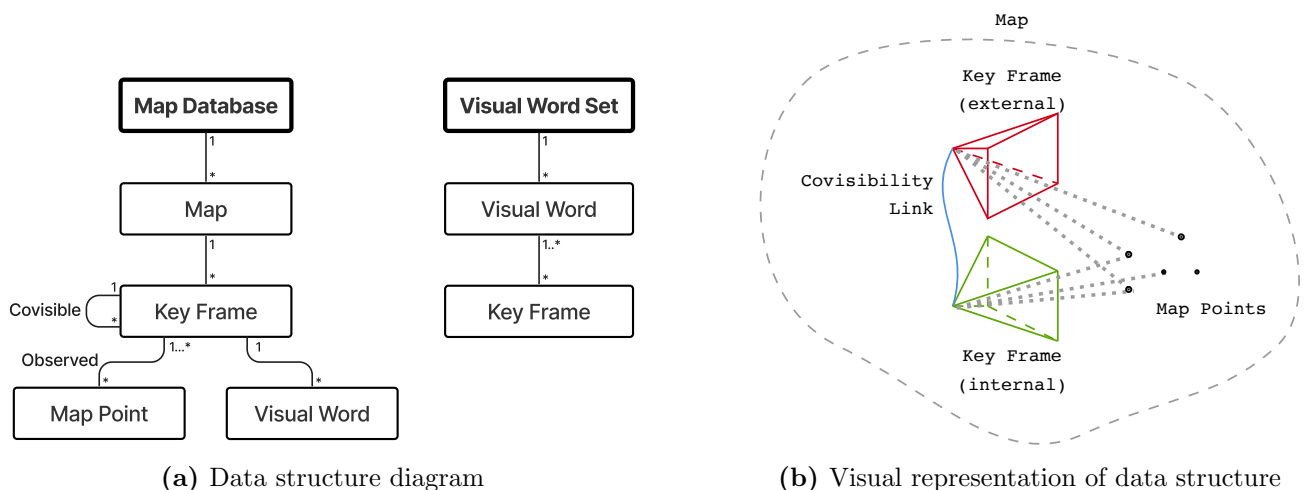
## 3.2 SLAM System

The SLAM System node is the majority of this project's implementation. It processes monocular images from the camera to localize the agent while also collaboratively building up a map of the world with its peers. As discussed in section 2.1, my system is based on an existing single-agent SLAM system that performs the **Tracking** and **Mapping** tasks. While substantial modifications were made to the base single-agent system, I will generally focus on the decentralized aspects of the system in the interest of space.

### 3.2.1 Data Structures

A brief discussion of my SLAM system's internal data structures is required to understand the following sections. Figure 3.2a shows the two key data structures: the map database and the visual word set. The map database contains multiple maps, which primarily consist of keyframes and map points. Keyframes are selected frames from the camera feed, containing the predicted pose of the agent at that time along with the observed world features which we call "map points". These map points can be observed by multiple keyframes, as shown in Figure 3.2b, and when this happens we connect the keyframes with a "co-visible" link.

Keyframes also have a "visual bag of words" representation, which is the vector describing the visual contents of the keyframe. These are essential for detecting potential map merges, so we also build a "visual word set" that allows us to find all keyframes that contain a particular visual word<sup>1</sup>.



<sup>1</sup>A "visual word" is a feature from the bag of words vocabulary.

### 3.2.2 Decentralized System Manager

Decentralized SLAM systems are significantly more complex than single-agent or even centralized systems, due to the nuanced interactions between agents as they merge maps, lose localization, or lose connection with their peers. Therefore, a robust framework must be put in place to ensure the correctness of the system, which I have implemented in the **Decentralized System Manager** component.

For the sake of simplicity, the next few sections will explore the interactions between just two agents: a *local* and *external* agent. In the Generalizing to  $N \geq 3$  Agent Systems section, we will show how this easily generalizes to a system with an arbitrary number of agents.

### 3.2.3 State Manager

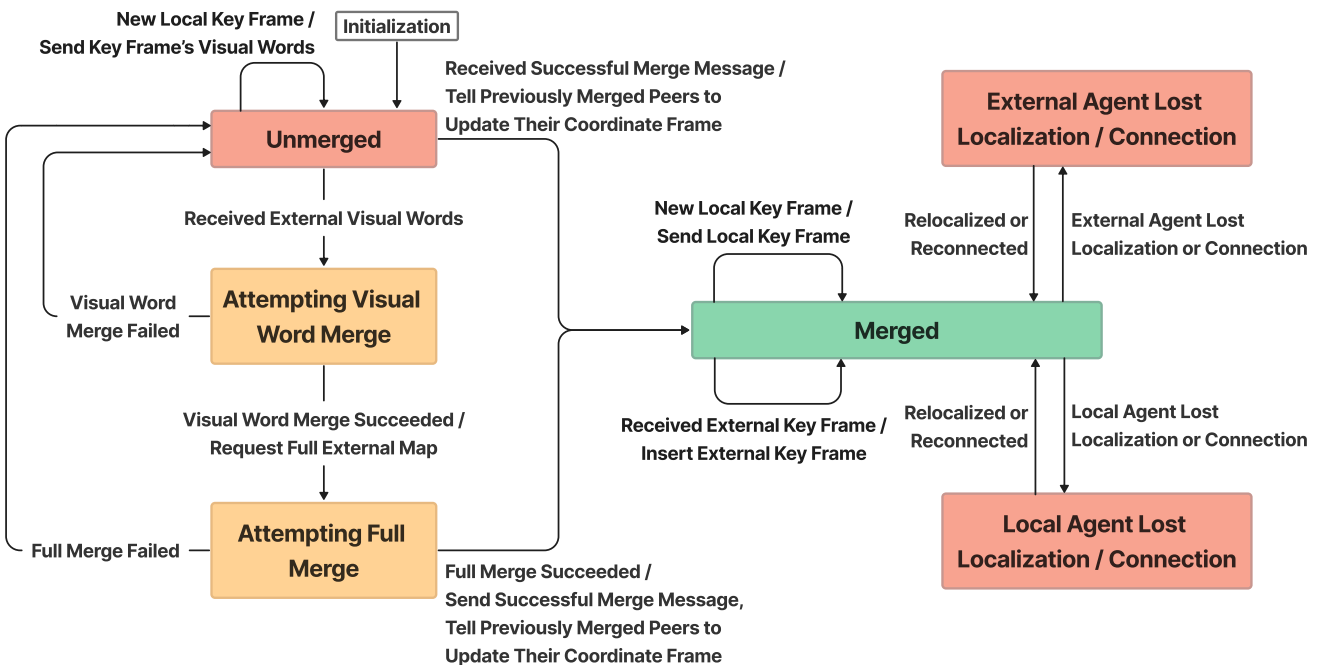


**Figure 3.3:** SLAM system state machine for a single peer. Mealy machine notation is used, where each transition is defined as: `input/output`.

Each agent's **Decentralized System Manager** maintains a state machine for every peer in the system, shown in Figure 3.3. All peers are initialized in the `unmerged` state, meaning that they are in different coordinate frames and share a unified map. As the local agent starts to explore the same locations as its peers, the system recognizes the visual overlaps and merges their maps, bringing us to the `merged` state where the agents share the same coordinate frame and map, enabling relative positioning and collaborative map building.

### 3.2.4 Map Serialization and Deserialization

Map serialization and deserialization are essential and non-trivial components of this SLAM system, enabling agents to share their maps across the network. For this task, I used the Boost Serialization C++ library [36] since it supports standard library collections and other common classes.

As discussed in section 3.2.1, maps contain keyframes and map points. Individually, these objects are relatively easy to serialize with boost – in fact, the single agent SLAM program my system is based on already supported saving and loading maps allowing me to leverage some

of their serialization helper functions. To serialize these objects we simply need to define a serialization scheme for each class, describing which instance variables should be serialized and which shouldn't.

Complexities arise when we try to serialize/deserialize the connections between these objects, especially when we are only sending map fragments as we may be required to "relink" deserialized objects with objects in our local map. We manage these connections by giving every keyframe and map point a universal unique identifier (UUID), allowing us to use these UUIDs as references to a specific object in our multi-agent system. We use UUIDs since they do not require a centralized server or any communication with our peers to assign a unique ID to every object<sup>1</sup>.

This method of using UUIDs as references is used to rebuild all connections after deserialization, including the keyframe-to-keyframe connections that build the co-visibility graph and many others that I have not had the space to discuss in this dissertation. A good example of connection rebuilding is later given in Figure 3.6, which shows how external map fragments are relinked with the local map.

### 3.2.5 External Map Merge Finder

A naive approach to merging our map with an external agent is to constantly exchange our full maps, each time trying to identify if a map merge is possible. While simple, this approach does not scale well from both a networking and computational perspective, as maps are often  $\geq 1\text{MB}$  in size, and computing a full map merge is extremely computationally expensive.

Instead, we first identify if a map merge is even feasible by using visual words. This eliminates superfluous map merge attempts that have no chance of succeeding because the agents' maps have no visual overlap.

As an agent generates new keyframes, we use DBoW2 [37] to calculate the visual bag of words seen by the keyframe and send them to our peers. These visual words are significantly smaller than sending over the complete keyframe (as shown in Figure 3.4) and enable agents to detect if there is a significant amount of visual overlap between its local map and the external agent's map.

Algorithm 3 is used to calculate if a merge is found by comparing the merge score of the external visual words to a dynamic baseline merge score, allowing the system to generalize to different environments. Algorithm 4 is the subprocedure used to calculate this merge score metric, giving a numerical value representing how well a visual bag of words "fits" into the local map. Notably, the algorithm exploits the spatial locality of keyframes which was found to give a more robust score.

This method gives a recall of almost 100%, at the cost of potentially lower precision. This is a worthwhile tradeoff, however, as it is essential to have very few false negatives so we can merge maps as soon as possible and the agents can begin collaborating.

---

<sup>1</sup>While not *verifiably* unique, UUIDs are unique within practical limits. A commonly cited anecdote is that it is far more likely for a cosmic ray to cause a bug than a UUID collision.

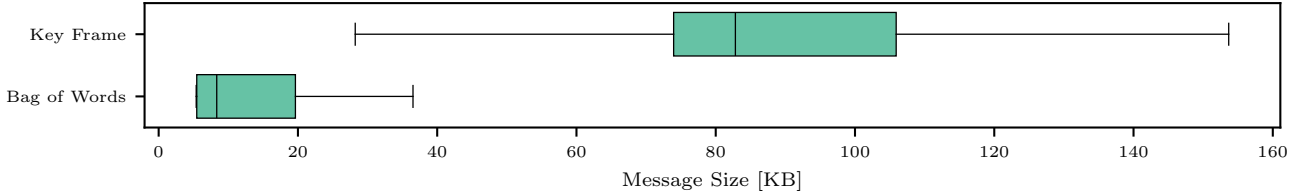


**Figure 3.4:** Comparison of the message size difference between a raw keyframe and a bag of words representation of a keyframe.

---

**Algorithm 3** Map merge finder using visual words.

---

**Input:**  $\text{VisualWords}_{ext}$ : Set containing external keyframe's visual words

**Output:** Success: Boolean value signaling if a merge is possible based on visual words

- 1:  $(\text{MergeScore}_{ext}, \text{BestMatchKeyFrame}) \leftarrow \text{CALCULATEMERGE SCORE}(\text{VisualWords}_{ext})$
  - 2:  $(\text{MergeScore}_{baseline}, \_) \leftarrow \text{CALCULATEMERGE SCORE}(\text{BestMatchKeyFrame}'s \text{ visual words})$
  - 3:  $\text{Success} \leftarrow \text{MergeScore}_{ext} \geq 0.7 \times \text{MergeScore}_{baseline}$
- 

**Algorithm 4** Calculate how well a bag of visual words merges with the local map.

---

```

1: procedure CALCULATEMERGE SCORE( $\text{VisualWords}$ )
2:   PotentialMatches  $\leftarrow$  query Visual Word Set data structure for similar keyframes
3:   BestMatchKeyFrame  $\leftarrow$  null
4:   BestMergeScore  $\leftarrow$  0
5:   for each  $\text{KeyFrame}_0$  in PotentialMatches do
6:     MergeScore  $\leftarrow$   $\text{KeyFrame}_0$ 's similarity to  $\text{VisualWords}$ 
7:     Covisible  $\leftarrow$  5 keyframes with highest covisibility with  $\text{KeyFrame}_0$ 
8:     for each  $\text{KeyFrame}_{cov}$  in Covisible do            $\triangleright$  Exploit spatial locality
9:       MergeScore  $+ =$   $\text{KeyFrame}_{cov}$ 's similarity to  $\text{VisualWords}$ 
10:    if MergeScore  $\geq$  BestMergeScore then
11:      BestMergeScore  $\leftarrow$  MergeScore
12:      BestMatchKeyFrame  $\leftarrow$   $\text{KeyFrame}_0$ 
return ( $\text{BestMergeScore}$ ,  $\text{BestMatchKeyFrame}$ )

```

---

### 3.2.6 External Map Merger

Once a potential map merge is found using visual words as described in the previous section, the external agent will send the local agent its full map and the local agent will attempt a full map merge using all the data.

Performing full map merges is perhaps the most important component of the decentralized SLAM system, as a bad map merge will make it impossible for agents to collaborate. Additionally, it is one of the most computationally intensive parts of this system, therefore, it has gone through numerous iterations to optimize performance and reduce map merge errors.

The final version of the map merger works as follows:

1. **Request external agent's full map.**

Once a potential map merge with the external agent is identified by the external map merge finder, we request its full map. Once the map is received, we deserialize it and temporarily place it into our `map database` data structure as a separate map.

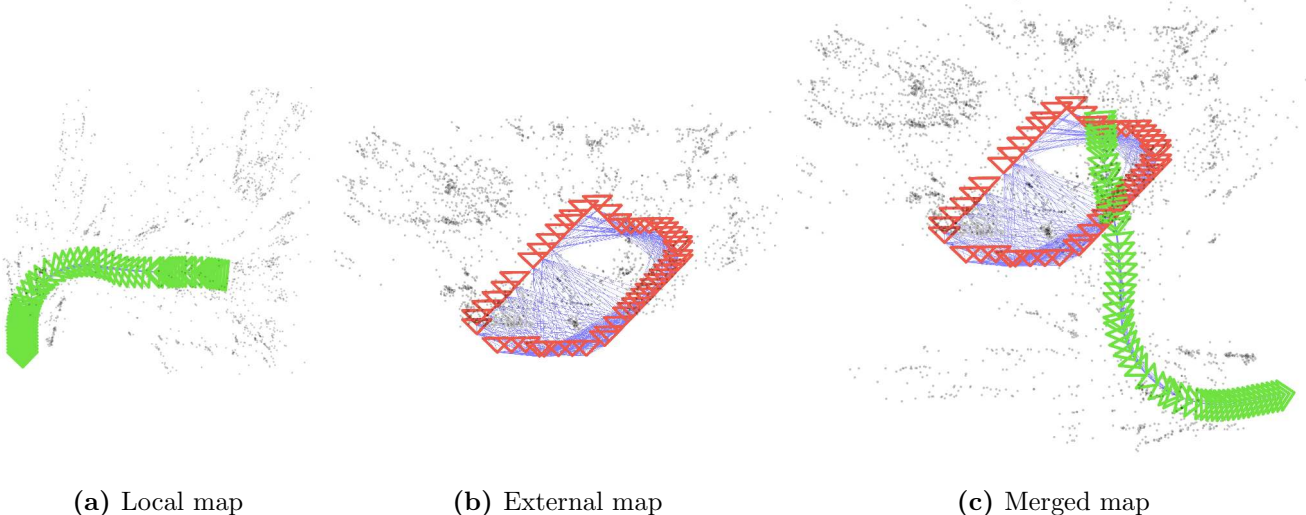


**Figure 3.5:** Visual overview of the map merge process. We apply the translation  $T_{loc \rightarrow ext}$  to the local map (a), and merge it with the external map (b), resulting in the merged map (c). The merged map contains information from both maps, creating our unified map. Note that the local map’s scale also needs to be transformed, due to the arbitrary scale of monocular SLAM systems.

## 2. Confirm that a map merge is possible using the full map data, and find the translation $T_{loc \rightarrow ext}$ that aligns the local map to the external map.

The visual word map merge finder identifies potential merges, however, we still need to confirm that a map merge is possible using the full map data from both agents. This is performed using a modified version of the ORB-SLAM3 loop closure detector.

If we determine the merge to not be possible, we delete the external map from our map database and exit this process.

## 3. Apply translation $T_{loc \rightarrow ext}$ to our local map.

This shifts the local agent to be in the external agent’s coordinate frame.

## 4. Move a subset of the external map’s keyframes and map points into our local map

Given the external keyframe  $k_0$  whose visual words triggered this map merge attempt, we extract a *local window*  $K_{wind}$  of keyframes connected to  $k_0$  in the co-visibility graph and move them to our local map. Moving only a small number of keyframes at first allows the map point merge and pose graph optimization process to be completed faster, which is important as they block local mapping from being performed.

## 5. Merge local and external map points, connecting the maps

## 6. Run pose graph optimization to optimize map point and keyframe positions.

## 7. Repeat steps 5-7 with the entirety of the external map.

## 8. Broadcast successful merge message.

If the full map merge is ultimately successful, we broadcast a `/successfully_merged` message to tell our peers that we have successfully merged with the external agent. The external agent will then move to the `merged` state and both agents will begin sharing keyframes with each other, allowing the external agent to receive the local agent’s full map.

It is important to note that this system requires only one agent to identify and calculate the map merge, significantly reducing the computational overhead of map merging, especially in systems with many agents (further explained in the Generalizing to  $N \geq 3$  Agent Systems section).

### 3.2.7 External KeyFrame Inserter

Once the local and external agents have merged their maps and are in the same coordinate frame, they can begin sharing keyframes with each other.

Each agent maintains a set of unsent keyframes  $K_{unsent}$  and map points  $M_{unsent}$ . Once  $\#K_{unsent}$  exceeds a certain threshold, we serialize  $K_{unsent}$  and  $M_{unsent}$  and send them to the external agent. Finally, we set  $K_{unsent} = \emptyset$  and  $M_{unsent} = \emptyset$ .

Upon receiving the serialized keyframes and map points, the external agent deserializes them and adds them to a queue to await insertion into their local copy of the shared map using the **external keyframe inserter**.

The external keyframe inserter is run whenever we have spare cycles on the CPU, to prevent impacting the local tracking and mapping performance. The insertion process involves the following operations:

(A concise visual overview of the process is presented in Figure 3.6)

1. **Pop  $k_{ext}$  from the front of the external keyframe queue.**
2. **Move  $k_{ext}$  and its external observed map points  $M_{ext}$  to the local map.**  
Since the local and external agents are merged, they are in the same coordinate frame. Therefore, we can move  $k_{ext}$  and  $M_{ext}$  to our local map without any transformations.<sup>1</sup>
3. **Relink  $k_{ext}$  with co-visible keyframes and observed map points in the local map.**  
 $k_{ext}$  contains references to its co-visible keyframes and child map points that have already been sent or were generated by another agent. We search our local map for objects that match these references, reconnecting them.
4. **Relink  $M_{ext}$  with keyframes in the local map which observe it.**  
 $M_{ext}$  contains references to keyframes that observe it which have already been sent or were generated by another agent. We search our local map for keyframes that match these references, reconnecting them.
5. **Merge  $M_{ext}$  with map points in the local map.**  
 $M_{ext}$  will already be correctly linked to observing keyframes in the local map from step 4., however, due to communication latency some map points in  $M_{ext}$  may be duplicates of existing map points in the local map. Therefore, we exploit spatial locality to merge duplicate map points that describe the same physical feature. A key observation from testing was that this step is essential to ensuring the local and external keyframes stay well connected, ensuring the local and external maps do not diverge.

---

<sup>1</sup>I had previously used a *keyframe anchor* method, where instead of  $k_{ext}$  having an absolute pose we would send its pose relative to the previous  $k_{ext}$ . The thought process behind this was to prevent minor misalignments between the local and external maps from preventing external keyframes from properly integrating with the local map. However, experimental testing showed that this method instead caused the local and external maps to frequently diverge.

## 6. Perform a local pose graph optimization around $k_{ext}$ .

This optimizes our map using the new information we received from the external agent.

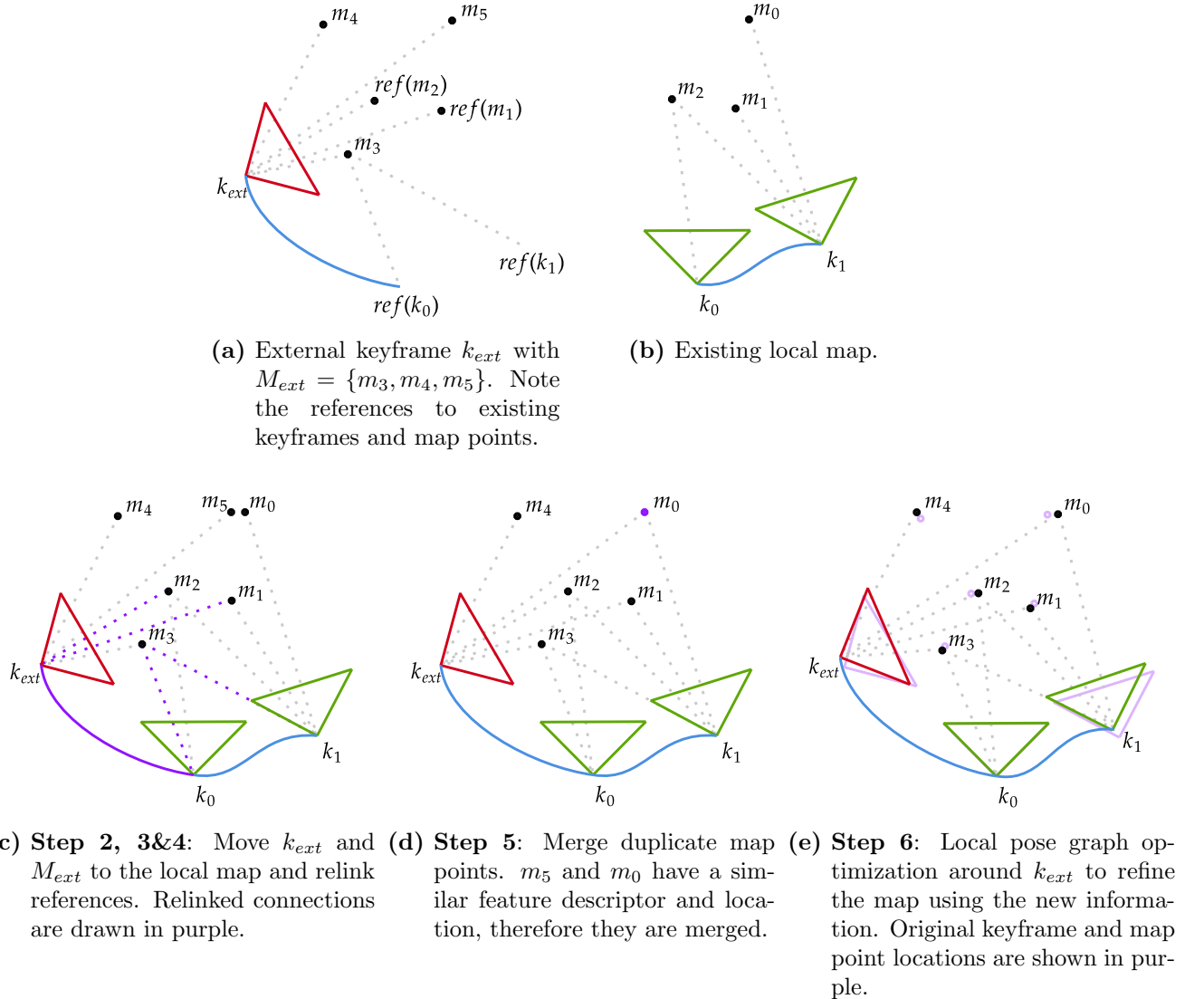


**Figure 3.6:** Visual overview of inserting external keyframes and map points into the local map. External keyframe (a) and initial local map (b) are combined to create our final local map (e).

### 3.2.8 Local KeyFrame Inserter

As mentioned in the External KeyFrame Inserter section, it is essential that the local and external maps stay well connected, sharing the majority of their map points. In other words, we must ensure that the external map data is integrated throughout the entire SLAM pipeline.

The **Tracking** and **Mapping** modules, which are responsible for localizing the robot and generating new keyframes, only interact with the **Map Database**, as seen in the previously shown architectural diagram in Figure 3.1. Our external keyframe inserter does all the work of properly reconnecting external map points and merging duplicate map points, leaving the **Map Database** data structure looking as if all the map points and keyframes were generated locally. This abstracts the **Tracking** and **Mapping** modules away from the distributed aspects of the system, ensuring that they fully utilize the external map points when localizing the agent and generating new keyframes (Figure 3.7).

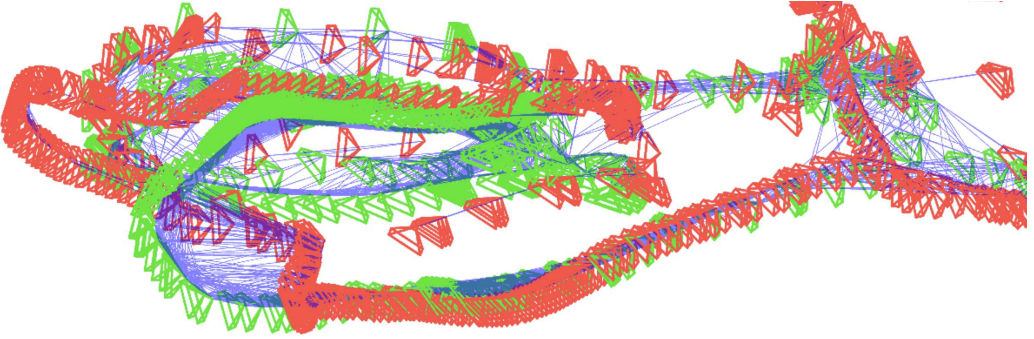


**Figure 3.7:** Section of the keyframes generated when running the EuRoC Machine Hall dataset. The local (green) and external (red) keyframes are well connected by co-visibility links (blue), demonstrating that they are tracking the same map points.

### 3.2.9 Generalizing to $N \geq 3$ Agent Systems

Now that we have explained how a pair of agents interact, we can explore how this can be generalized to a system with an arbitrary number of agents.

We assume a system with  $N$  agents  $A = \{agent_1, agent_2, \dots, agent_N\}$ , where  $agent_i$  is the agent with ID = i. Within this system we maintain a state  $S_i = state_{n-m}$  for every agent pair  $(agent_n, agent_m)$ , giving us a total of  $N(N - 1)/2$  states. We also have a set  $G$  which contains all the groups of merged agents. The *group leader* is defined as the agent in a group with the lowest agentId.

In the case where agents can lose communication with one another, we also assume that if any given  $agent_n$  is able to communicate with an  $agent_m$ ,  $agent_n$  can also communicate with all of  $agent_m$ 's connected peers. This is held if the agents are using a mesh network to communicate, for example.

Initially, every agent pair is unmerged so every state in  $S$  is set as *unmerged* and  $G = \{\{agent_1\}, \{agent_2\}, \dots, \{agent_N\}\}$

A key insight of my distributed SLAM system is to delegate all merge operations to group leaders. This is significant, as the computational load and bandwidth requirements of these merge operations scale proportional to the square of the number of agents involved, and in most use cases the number of group leaders quickly drops to be much lower than the total number of agents. Additionally, having all merge operations performed by the group leader prevents potential race conditions introduced by communication latency within a group, for example, two agents within a group merging with different agents at the same time.

As discussed in the External Map Merge Finder and External Map Merger sections, the two operations needed to merge are (1) exchanging visual words to identify visual overlap and therefore merge opportunities and (2) sending over the map and attempting a full map merge. Our group leaders must therefore perform these tasks on behalf of their groups.

The “visual word merge finder” operation can be delegated to group leaders by having them send the visual words of all keyframes generated by agents within their group to all other group leaders. This introduces no additional intra-group communication, as all agents within a group already send each other all new keyframes.

Moving on to the “full map merge” operation, once a pair of group leaders ( $agent_n, agent_m$ ) (with  $n < m$ ) have found a potential merge using visual words, the agent with the smaller

ID ( $agent_n$ ) sends its full map to the agent with the larger ID ( $agent_m$ ), who attempts a full map merge. If the merge is successful,  $agent_m$  will now be in  $agent_n$ 's coordinate frame.  $agent_m$  will then send the transform from  $agent_m$  to  $agent_n$ 's coordinate frame  $T_{m \rightarrow n}$  to all the agents in its group, allowing them to also change to  $agent_n$ 's coordinate frame. After this has been completed,  $agent_m$ 's group merges into  $agent_n$ 's group by updating  $S$  according to Equation 3.1, and agents begin exchanging keyframes to update the unified map.

$$\forall i \in g_n. \forall j \in g_m. state_{i-j} \in S \text{ and } state_{i-j} = \text{"merged"} \quad (3.1)$$

where  $g_n, g_m \in G$  are the groups that  $agent_n$  and  $agent_m$  respectively lead.

This approach requires all agents to know the current groups and group leaders within the decentralized system, which is achieved by broadcasting all successful merge messages on the `/successfully_merged` ROS topic for everyone to see.

This whole process is perhaps best represented in visual form by the simple 3-agent merge example given in Figure 3.8 which shows the messages sent between agents.

### 3.2.10 Map Alignment Refiner

As our shared map grows, our local map may “fall out of alignment”. In other words, the map is slightly translated, rotated, or scaled with respect to the lead agent’s map. This is largely a side effect of our aggressive early merge strategy which may merge two agents’ maps before there is significant overlap, causing the estimated map alignment to have some error. These small alignment errors are completely acceptable when maps are small, but may cause the maps to diverge as they grow.

To remedy this problem, we continuously refine our map alignment using the RANSAC and Kabsch-Umeyama point set alignment algorithms. Map alignment is performed as follows:

- 1. Request map point locations from the lead agent.**

This is defined as the set  $\text{TaggedMP}_{ext}$  where  $\text{TaggedMP}_{exti} = (\text{uuid}, (x, y, z))$

- 2. Extract local map point locations.**

This is defined as the set  $\text{TaggedMP}_{local}$  where  $\text{TaggedMP}_{locali} = (\text{uuid}, (x, y, z))$

- 3. Use RANSAC with the Kabsch-Umeyama algorithm to find the transform  $T_{local \rightarrow ext}$  which best aligns  $\text{TaggedMP}_{local}$  to  $\text{TaggedMP}_{ext}$ .**

The Kabsch-Umeyama algorithm finds the  $\text{SIM}(3)$  transformation  $T_{local \rightarrow ext}$  from  $\text{TaggedMP}_{ext}$  to  $\text{TaggedMP}_{local}$ , minimizing the root mean squared error. However, our input data may contain a large number of outliers so we use RANSAC to find a good fit while ignoring outliers.

- 4. Apply transformation  $T_{local \rightarrow ext}$  to our local map to realign it with the group leader.**

We use an *additive increase multiplicative decrease* methodology to control how often map alignment is performed. Given  $t_i$  is the time between the  $i$ -th and  $(i + 1)$ -th map alignments, we set  $t_{i+1} = t_i + 1$  if the maps were well aligned, and  $t_{i+1} = t_i/2$  if the maps were not well aligned. This prevents agents from continuously performing map alignments when their maps are already well aligned.

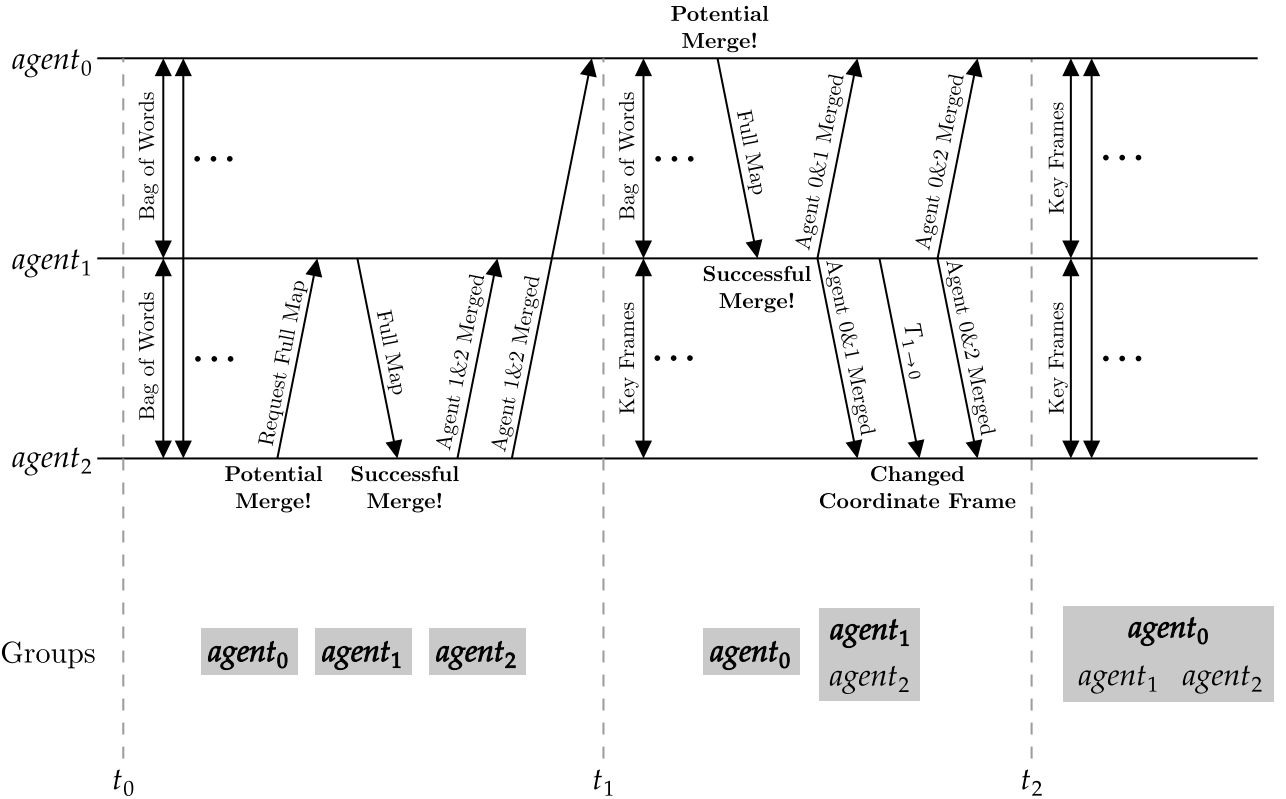


**Figure 3.8:** This is a simple 3 agent merge example where  $agent_1$  and  $agent_2$  merge first, and then  $agent_0$  and  $agent_1$ . Agents in the same group are shown in the same rectangle, with the group leaders bolded.

Initially at  $t_0$ , all agents are unmerged. Therefore, they are all group leaders and share the “bag of words” representations of new keyframes with each other.  $agent_2$  then finds a potential merge with  $agent_1$ . The lower agent ( $agent_1$ ) sends  $agent_2$  its full map, who successfully merges with it, transforming it into  $agent_1$ ’s coordinate frame.

At  $t_1$ ,  $agent_1$  and  $agent_2$  are merged and therefore begin exchanging keyframes.  $agent_0$  and  $agent_1$  are the two remaining group leaders, so they continue to exchange their “bag of words”.  $agent_0$  detects a potential merge with  $agent_1$ , and since  $0 < 1$  it sends its full map to  $agent_1$ .  $agent_1$  successfully merges with  $agent_0$ ’s full map, so it sends the transform  $T_{1 \rightarrow 0}$  ( $agent_1$  to  $agent_0$ ’s coordinate frame) to all members of its group. This allows  $agent_2$  to change from  $agent_1$  to  $agent_0$ ’s coordinate frame.

At  $t_2$ , all three agents are merged and in  $agent_0$ ’s coordinate frame. Therefore they all exchange keyframes with one another.

This example is slightly simplified as all potential merges result in successful full merges. In reality, multiple potential merges may be identified before two agents successfully merge.

### 3.2.11 Losing Localization / Connection

An agent can lose localization within the shared map (for example, if its camera is blocked for a short period of time). When this happens, the agent signals to its peers that it has lost localization and they stop sharing new keyframes. Since the agent has lost localization in the shared map, it begins building a private map of the new area it is observing. If it revisits an area of the shared map, it will merge its private map with the shared map and signal to its peers that it has regained localization. Keyframe sharing will then resume, with the agents’ unsent

keyframes being sent to one another. This allows the new area explored while localization was lost to expand the shared map.

Losing connection is very similar, however, a new private map does not need to be built. Instead, the agents simply stop sharing keyframes until the connection is regained, at which point the agents will update each other with the stored-up unsent keyframes.

### 3.2.12 Visualization Publisher

All 3D visualizations are created by publishing ROS markers, a standardized ROS message type that represents some object in 3D space such as lines, points, or meshes. These ROS markers can then be displayed by a variety of third-party visualization tools such as RViz [38] and Foxglove Studio [39].

Using ROS markers allows me to leverage these mature visualization tools instead of creating one from scratch, and also allows visualizations to be easily saved and replayed for later analysis. Demonstrations of these 3D visualizations can be found in the supplementary video<sup>1</sup>

## 3.3 Motion Controller

While not a part of the core SLAM system, the motion controller node closes the control loop and provides real-world demonstrations of my system. From a high level, the motion controller node consumes the local and external agents' poses and outputs a command velocity to the robot's movement system – all via ROS topics. For this project, I have implemented two different motion control systems which can be switched between seamlessly.

### 3.3.1 Follow The Leader

The *follow the leader* motion controller consists of two agents: one leader and one follower. The follower is given a position and rotation offset to the leader which it attempts to maintain as the leader is moved around.

### 3.3.2 Multi-Agent Collision Avoidance

The *multi-agent collision avoidance* example is more complex, employing a non-linear model predictive controller (NMPC) to avoid collisions with both static and dynamic obstacles. My NMPC system is improved version of [40] and is defined as follows:

#### 3.3.2.1 Non-Linear Model Predictive Controller Formulation

We assume an agent with current pose  $\mathbf{p} \in \mathbb{R}^2$  and radius  $r$ . Firstly, we define our agent's control input  $\mathbf{v}_{cmd}$  as a function describing its velocity over time. We can then define our agent's state as a function of time  $\mathbf{x}(t)$  as the control input  $\mathbf{v}_{cmd}$  applied to its current pose  $\mathbf{p}$ :

$$\mathbf{x}(t) = \mathbf{p} + \int_0^t \mathbf{v}_{cmd} dt \quad (3.2)$$

---

<sup>1</sup>Supplementary video URL: <https://cam-diss.s3.amazonaws.com/video.mp4>

Solving the following minimization problem will yeild an optimal  $\mathbf{v}_{cmd}$ :

$$\begin{aligned} \min_{\mathbf{v}_{cmd}} & \int_{t=0}^T J_x(\mathbf{x}(t), \mathbf{x}_{ref}(t)) + J_s(\mathbf{x}(t)) + J_d(\mathbf{x}(t)) dt \\ \text{subject to } & \mathbf{v}_{min} \leq \mathbf{v}_{cmd} \leq \mathbf{v}_{max} \end{aligned} \quad (3.3)$$

where  $T$  is our horizon length,  $\mathbf{x}_{ref}$  is our target trajectory, and  $J_x$ ,  $J_s$ ,  $J_d$  are the cost functions for this system.

Cost function  $J_x$  rewards following the target trajectory  $\mathbf{x}_{ref}$  and is shown below:

$$J_x(\mathbf{x}, \mathbf{x}_{ref}) = \|\mathbf{x} - \mathbf{x}_{ref}\|^2 \quad (3.4)$$

$J_s$  and  $J_d$  penalize collisions with static objects and dynamic objects respectively. They are defined as:

$$J_s(\mathbf{x}) = \sum_{i=1}^{N_{static}} \frac{s_s * Q_s}{1 + \exp(d_i^{static}/s_s)} \quad (3.5)$$

$$J_d(\mathbf{x}) = \sum_{i=1}^{N_{dynamic}} \frac{s_d * Q_d}{1 + \exp(d_i^{dynamic}/s_d)} \quad (3.6)$$

where  $d_i^{static}$  is the distance between the agent and the  $i$ -th static obstacle, and  $d_i^{dynamic}$  is the distance between the agent and the  $i$ -th dynamic obstacle.  $Q_s > 0$  and  $Q_d > 0$  are weights that define how adverse our agents are to collision with static and dynamic obstacles respectively. A visualization of how these parameters affect the cost function is presented in Figure 3.9a.

Additionally, we define  $s_s$  and  $s_d$  as scale normalizing parameters that ensure the minima of  $J_x + J_s$  and  $J_x + J_d$  are invariant to  $Q_s$  and  $Q_d$ . To calculate  $s_s$ , we first find the positive minima  $x_{min}$  of  $J_x + J_s$  in the worst case where  $d_i^{static} = J_x$  (ie. the static obstacle and  $x_{ref}$  are at the same place), with  $s = 1$ . This gives us  $x_{min}$  as defined in Equation 3.7. Our scaling factor can then be defined as  $s_s = \frac{r}{x_{min}}$ , which sets the positive minima of  $J_x + J_s$  to be  $r$  in the above situation. The calculation of  $s_d$  is symmetric, simply using  $Q_d$  instead of  $Q_s$ .

$$x_{min} = \ln \left( \frac{\sqrt{Q_s^2 - 4Q_s} + Q_s}{2} - 1 \right) \quad (3.7)$$

The key benefit of these cost functions is that the optimal distance to obstacles is kept at the collision point, and is invariant to parameters  $Q_s$  and  $Q_d$ . This is in contrast to [40] which requires the parameters  $\kappa$  and  $Q$  to be re-tuned after changing agent radius  $r$ . This is because their cost functions do not have their minima at the collision point, but instead at some point before the collision that varies with  $\kappa$ ,  $Q$ , and  $r$ , making them very difficult to tune. This is visualized in Figure 3.9

### 3.3.2.2 Implementation Details

Solving the integral in Equation 3.3 is computationally inefficient, therefore we split our calculations into discrete time steps. Specifically, the time horizon is set as  $T = 500ms$  with  $100ms$  timesteps.

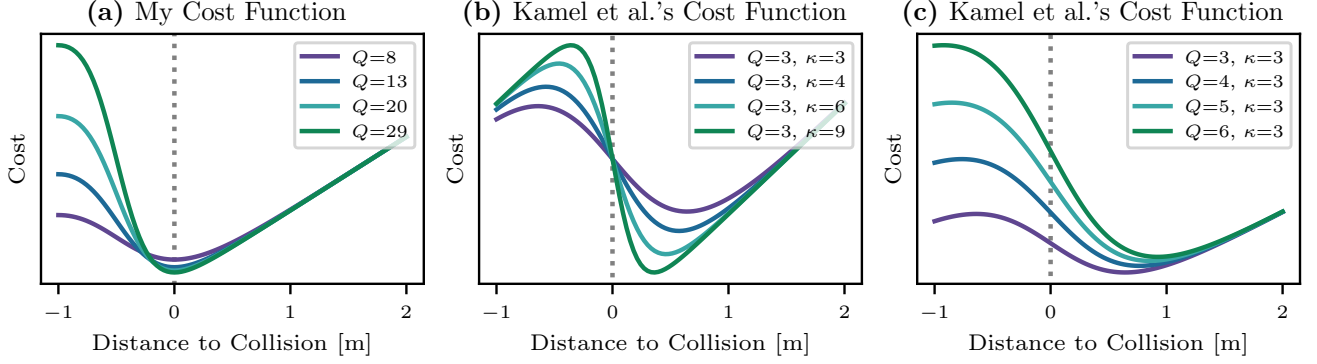


**Figure 3.9:** Comparison of my cost function (a) and Kamel et al.’s cost function (b), (c) when the obstacle and goal pose are at the same location. This demonstrates that my cost function’s minima is always at the collision point and does not vary as the parameters are changed, as opposed to Kamel et al.’s function.

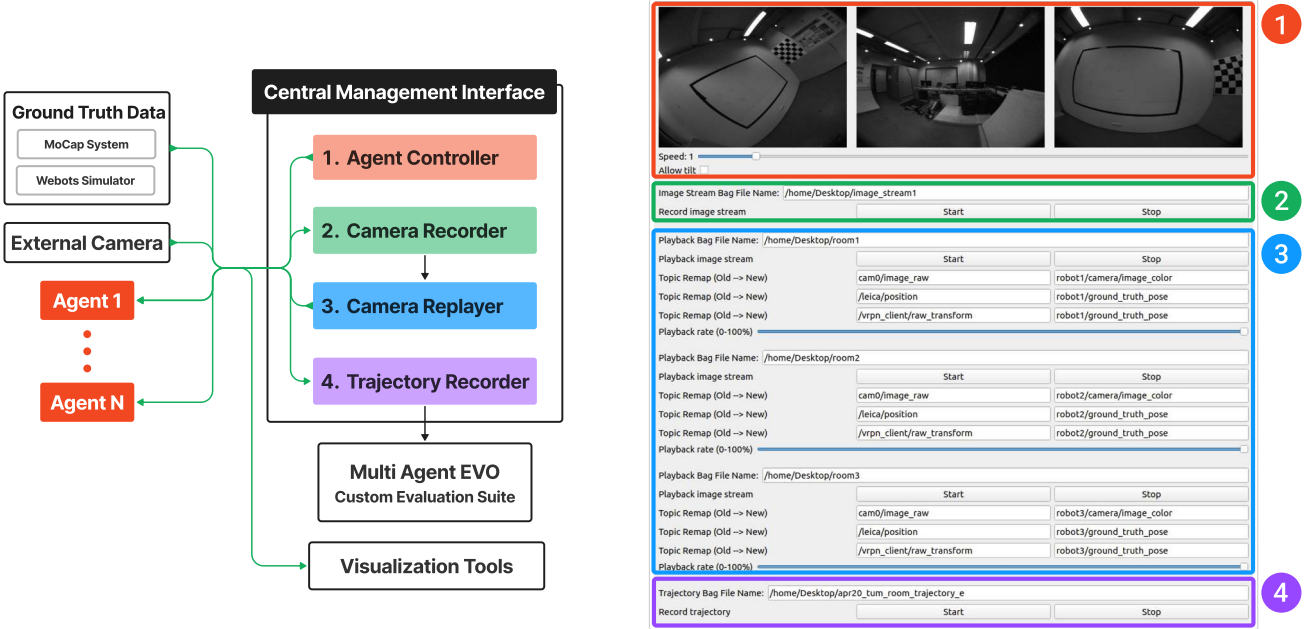
The *Sequential Least Squares Programming* minimization method is used due to its robustness and ability to constrain the optimization space, which we use to keep  $\mathbf{v}_{min} \leq \mathbf{v}_{cmd} \leq \mathbf{v}_{max}$ . We set parameters  $Q_s = 8$  and  $Q_d = 12$  to make the agent more adverse to approaching dynamic obstacles than static ones, as there is more uncertainty in the dynamic obstacle’s location. To calculate the future locations of dynamic obstacles  $\mathbf{x}_i^{dynamic}(t)$  we employ a simple constant velocity model.

## 3.4 Central Management Interface

While my multi-agent system is fully decentralized, a significant amount of work was put into developing the supporting infrastructure needed to control, test, and evaluate this system. The primary method of managing the distributed system is through the cross-platform *Central Management Interface*, which can be used to:

1. **Manually control the agent’s poses.**  
Users can click and drag on an image in area 1 to rotate the agent’s camera and use the keyboard to move the agent around.
2. **Record camera data from the simulation software.**
3. **Play datasets back for testing and benchmarking purposes.**
4. **Record trajectories generated by the SLAM system as well as ground truth data for later evaluation.**  
The recorded trajectory data can later be ingested by my custom evaluation library Multi-Agent Evo for analysis.

As a result of abstracting implementation details behind ROS topics, this central management interface is able to work seamlessly with both agents running in a simulator and agents running on real-world robots.



(a) Central Management Interface architectural diagram

(b) Central Management Interface

**Figure 3.10:** The central management interface, used for controlling agents, recording datasets, playing back datasets, and recording trajectories for later analysis.

### 3.5 Custom Evaluation Suite – Multi-Agent EVO

While there are several mature single-agent SLAM evaluation tools, I found there to be a complete lack of evaluation tools for multi-agent SLAM systems – to the best of my knowledge no papers have published their evaluation code. Therefore, I have created an open-source multi-agent SLAM evaluation tool: *Multi-Agent EVO*, based on the popular single-agent SLAM evaluation tool *EVO* [41].

In addition to the data structures and data ingestion modifications needed for EVO to process multi-agent SLAM data, evaluating data from a multi-agent system introduces some additional complexities.

Initially, all agents are in separate reference frames until they merge their maps and begin sharing the same coordinate frame. We may also have cases where two independent groups of agents meet and merge maps, which requires multiple agents to simultaneously change coordinate frames.

Therefore, I have created a new data format to capture these changes in coordinate frames over time within our trajectory data, which Multi-Agent EVO is able to ingest. This allows us to properly compare the multi-agent SLAM trajectories to the ground truth data, giving us insights into how long it takes for agents to successfully merge maps, the accuracy of relative pose estimation, and much more.

Once agents  $m$  and  $n$  merge, they publish the translation  $T_{m \rightarrow n}$  to the `sim3_transform` ROS topic. When we go to evaluate the trajectory error, Multi-Agent EVO ingests the `sim3_transform` data to build a directed acyclic graph (DAG) of all merged agents, as shown in Figure 3.11. This DAG can then be used to find if agents are merged with each other, and the transform between their coordinate frames. We then transform all the trajectories to be in  $agent_0$ 's coordinate frame for us to perform error analysis on the joint trajectory.

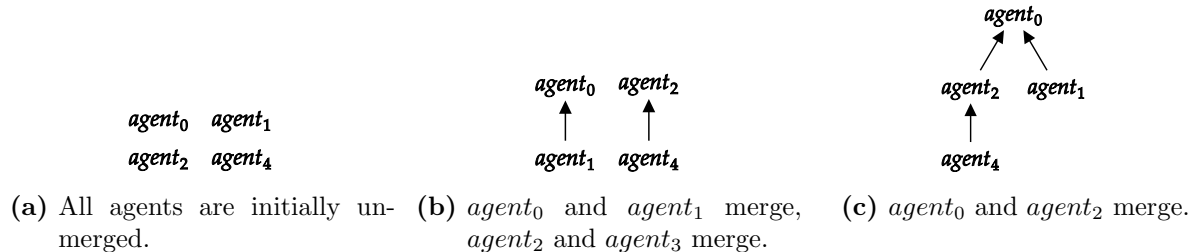


**Figure 3.11:** Example of how coordinate frames are managed in Multi-Agent EVO. A path from  $agent_m$  to  $agent_n$  signifies that the agents are merged and there is an available translation from  $agent_m$ 's coordinate frame to  $agent_n$ 's.

This method also allows us to retroactively transform trajectories into  $agent_0$ 's coordinate frame before the agents merged, allowing us to analyze the error of the pre-merge estimated relative trajectories.

## 3.6 Simulation Environment

The Webots Simulation Software section in the Preparation chapter explains the motivation behind using a simulator. Essentially, leveraging simulations enables much faster iterations and the ability to test my system in a variety of environments. This section will focus on the details of integrating the simulation software into my system.

Webots [31] is an open-source 3D robotics simulator with realistic rendering, which is essential for testing a visual SLAM system. Unfortunately, Webots can not be built for the ARM Ubuntu VM I used for development, therefore it had to be run on MacOS, with data being streamed to the Ubuntu VM through a websocket bridge developed by Webots.

I have developed a ROS node that exposes the Webots camera and agent controls as ROS topics, following the abstract robot interface specifications. This allows my SLAM system to process the camera streams, and the motion controller / central management interface to control the agent's velocity in the simulated environment.

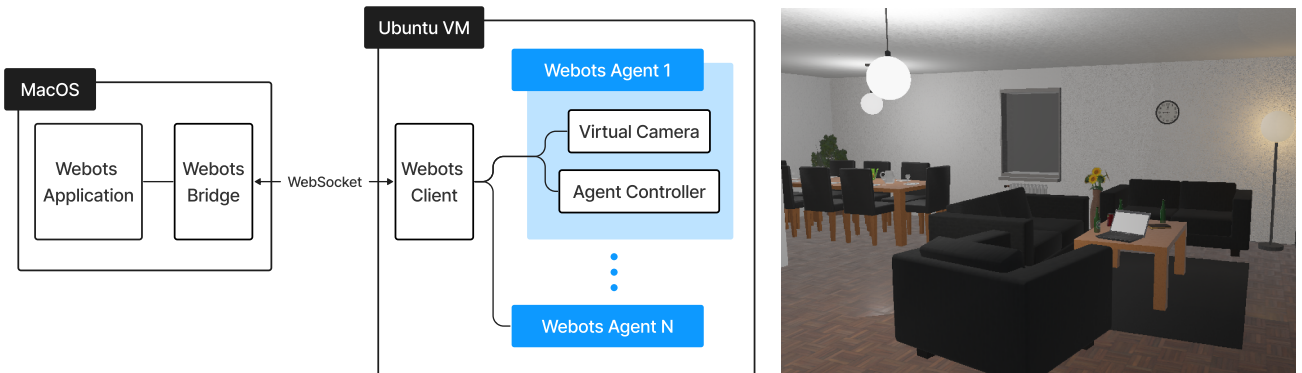


**Figure 3.12:** Simulation system architecture. The Webots application runs on MacOS and is exposed to the Ubuntu VM as ROS topics by the custom Webbots Client ROS node.

**Figure 3.13:** Webots render of the “Apartment” environment.

## 3.7 Real World Implementation

After months of development within a simulator, my distributed SLAM system was able to seamlessly be deployed to a real-world multi-agent system. This was largely due to the decisions

made during the preparation phase. For example, the choice to use ROS as a communication middleware allows the agents to easily communicate, even when deployed on different physical devices. Another key choice was to abstract the implementation of nodes away behind the communication layer, as it allowed my system to interface with the physical robots without needing to make any changes to the SLAM system or motion controller nodes.

### 3.7.1 Cambridge RoboMaster Platform

I chose to deploy my system on the Cambridge RoboMaster, which is an omnidirectional robot platform with a NVidia Jetson Orin for compute (Figure 3.15). The only sensor used on the RoboMaster was the integrated Raspberry Pi HQ Camera, which provides a 1920x1080 image at 15hz. This was an obvious platform to use as ROS drivers for the camera and wheels had already been developed and a ground-based platform allows for easier testing.

As explained in the Docker and Continuous Integration / Continuous Deployment section, my system is compiled in the cloud and deployed on the robots in Docker containers.

As an aside, I was an author of the paper *The Cambridge RoboMaster: An Agile Multi-Robot Research Platform* [4], which has been submitted to the 17th International Symposium on Distributed Autonomous Robotic Systems. My distributed SLAM system was included in the paper, with my system being run in conjunction with my multi-agent collision avoidance motion controller to evaluate the robotics platform's performance and capabilities.

### 3.7.2 OptiTrack Motion Capture System

The ground truth for my real-world experiments is provided by the Prorok Lab's OptiTrack Motion Capture System, which advertises accuracies of  $\leq 0.3\text{mm}$  at rates of 180hz [42]. The motion capture system publishes the real-time poses of the tracked objects to a ROS topic which can be recorded for later analysis.

### 3.7.3 Raspberry Pi Video Publisher

This dissertation also presents the Raspberry Pi Video Publisher, an independent piece of infrastructure which I have developed both the hardware and software for. This platform publishes real-time camera data to a ROS topic and can be tracked by the lab's motion capture system. The two primary use cases for this platform are (1) dataset generation and (2) real-time AR visualization of 3D data (section 3.7.4).

The hardware for this platform consists of a Raspberry Pi 4b, Raspberry Pi Camera v2, 3D printed frame, and motion capture markers. The 3D-printed frame securely mounts the components together, allowing the system to be carried around or mounted to a tripod as shown in Figure 3.14.

ROS does not support streaming videos across a network, instead requiring frames to be sent as individual compressed images. This results in significant computational overhead, with a naive ROS video publisher implementation only being able to stream at 10 frames per second on the Raspberry Pi. To enable a 30-frame-per-second video stream, my implementation uses three threads. The first thread captures images from the camera, the second encodes them as a JPEG image, and the third publishes the images to a ROS topic.

As explained in the Docker and Continuous Integration / Continuous Deployment section, the software for this platform is entirely dockerized and a CI/CD pipeline has been implemented to

automatically build and deploy the software to all Raspberry Pi video publishers when new code is pushed to the GitHub repository. The ease of use of the Raspberry Pi ROS video publisher platform has made them an invaluable tool and resolves the time-syncing issues previously faced when using the existing cameras in the Prorok Lab.

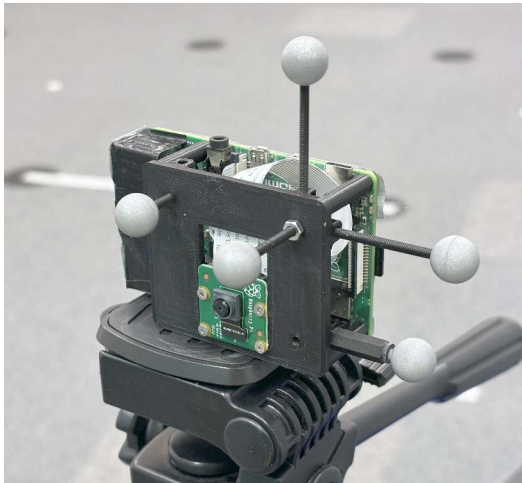


**Figure 3.14:** Custom-built Raspberry Pi Video Publisher mounted on a tripod.



**Figure 3.15:** Cambridge RoboMaster platform with NVidia Jetson Orin and Raspberry Pi HQ Camera.

### 3.7.4 Augmented Reality Visualization

The Raspberry Pi Video Publisher platform is tracked by the motion capture system, allowing us to project 3D visualization data onto the captured video. This can be used to visualize the SLAM system's keyframe and map point locations in the real world and to view how the predicted trajectory aligns with reality.

To overlay this data on the video, we must first align the SLAM system and motion capture systems' coordinate frames. This needs to be done on every run, as monocular SLAM systems have an arbitrary scale. Therefore, we use the Kabsch-Umeyama Algorithm to align the trajectories captured by the motion capture system and SLAM system after enough data has been collected to create a successful alignment. We can then use Foxglove Studio to draw our 3D markers and project them on top of the tracked camera's video stream, a snapshot of which is displayed in Figure 3.16.

Importantly, the tool is built around the standard ROS marker interface. This makes it a generic platform that can give an AR visualization of any experiment being conducted in a motion capture environment.

To my knowledge, this system is the first of its kind to be used in such a project. Not only is it visually impressive, but it also can be used for further analysis and understanding. For example, this visualization helped me identify that my collision avoidance demo was being severely impacted by latency spikes which I proceeded to fix.



**Figure 3.16:** Features tracked by the RoboMaster overlaid over an “external perspective” handheld video from my Raspberry Pi Video Publisher. This visualization makes it clear that my SLAM system is tracking the corners of boxes, letters on the Prorok Lab banner, and the floor vents.

Note that the features are generated by the RoboMaster, and then reprojected onto the video captured by the Raspberry Pi as it moves through space. This is made clear in the video demonstration of this feature at 2m07s of the supplementary video<sup>1</sup>.

## 3.8 Repository Overview

My dissertation consists of five ROS packages, a Python library, 3D designs, and dozens more miscellaneous files, amounting to **35,000+ lines of code** across **108 files** and **three repositories**. While lines of code and number of files are a poor measurement of complexity, I still hope to illustrate the scale of this software engineering project. The following section gives a brief overview of my codebase’s structure.

The `distributed_visual_slam` repository (Figure 3.17) contains the core SLAM system and all the infrastructure needed to run it. This includes five ROS packages: `slam_system`, `motion_controller`, `webots_sim`, `central_management_interface`, and `interfaces`, which all follow the standard ROS package structure. `slam_system` and `interfaces` are written in C++ and built using CMake, while the remaining packages are Python-based.

The `rpi_ros2_camera_publisher` repository (Figure 3.18) holds the code, 3D files, and CI/CD configuration for the Raspberry Pi Camera Publisher system. The provided Systemctl service file configures the Raspberry Pi to pull and run the latest docker image on startup.

The `multi_agent_evo` repository (Figure 3.19) is a modified version of the EVO library [41] that supports the evaluation of multi-agent SLAM systems.

---

<sup>1</sup>Supplementary video URL: <https://cam-diss.s3.amazonaws.com/video.mp4>

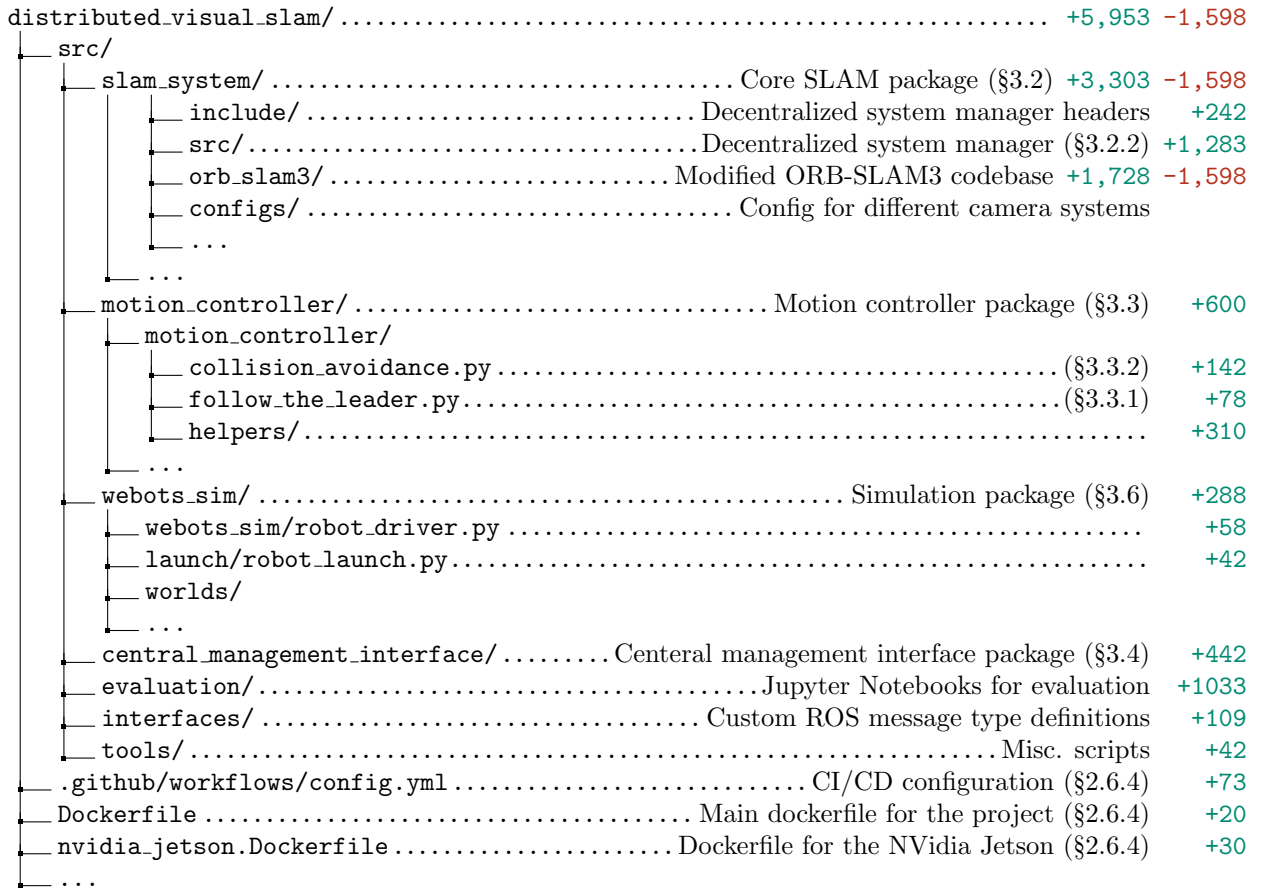


**Figure 3.17:** Repository overview for my distributed visual SLAM system. Line count does not include non-code files (e.g. camera configurations, simulation worlds, et cetera.)

`git diff` is used for the `orb_slam3` folder, as it is a fork of an existing single-agent SLAM system [5]. The `git diff` excludes reformatting and the mass deletion of unused files.

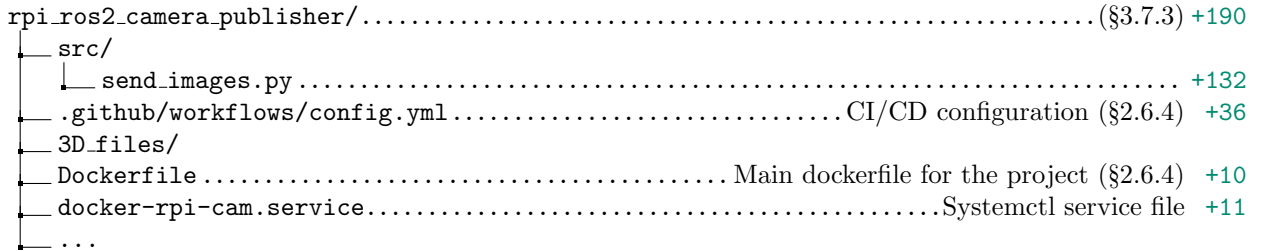


**Figure 3.18:** Repository overview for the Raspberry Pi Camera Publisher system.

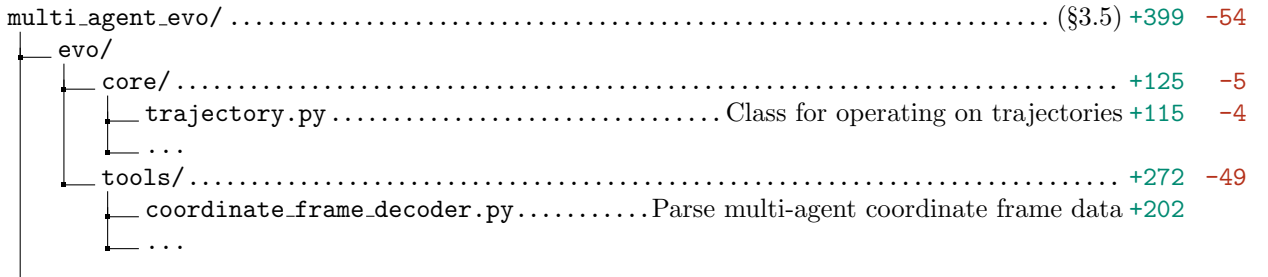


**Figure 3.19:** Repository overview for the Multi-Agent EVO evaluation library.

Note that a `git diff` is given for the repository, as it is a fork of the single agent evaluation library EVO [41].

# Chapter 4

## Evaluation

### 4.1 Review of Success Criteria

My project has met all success criteria as outlined below. Their success is substantiated by the subsequent sections in this chapter.

**1a. Multiple agents will be able to localize themselves within a world using purely visual data.**

My dissertation presents a novel decentralized SLAM system capable of operating using only monocular camera data. This removes the need for large and expensive stereo cameras, LiDAR, or RGBD sensors.

**1b. Agents will be capable of communicating with each other to build a shared understanding of the world.**

Agents are capable of efficiently computing map merges and exchanging keyframes to build a shared map of the world. This map can subsequently be used to provide the relative position of peers, as is shown in the real-world collision avoidance experiments.

**1c. Agents will be able to act independently, failing gracefully if they lose communication with their peers.**

Agent autonomy is implicitly built into my distributed framework. When communication is degraded, agents will store up map data and send it when communication resumes. This goal is extended by allowing agents to fail gracefully if localization is lost.

**2. Evaluate the capabilities of the system compared to a comparable single-agent system.**

This is performed in the Benchmarking section. I go beyond the original success criteria by also comparing my system to comparable multi-agent systems, demonstrating my system's superior performance.

After discussions with my supervisor, we decided to not pursue my original project extensions<sup>1</sup>, as we believed that they had either implicitly been achieved during the development of my core deliverables or were no longer relevant to my project.

More importantly, however, we were convinced that deploying my system on to physical robots would have far more potential, and in retrospect, I believe that we made the correct choice. Operating my system in real-time on a distributed platform proves its applicability in real-world scenarios, and shows that my system can adapt to the noisy and unpredictable conditions of the real world, greatly improving its credibility. Moreover, deploying my system on to the Cambridge RoboMasters provides evidence of how my software engineering choices have enabled my system to be reproducible on a variety of hardware, instead of just my laptop.

### 4.2 Benchmarking

This section will benchmark the performance of my system when run on industry-standard visual SLAM datasets. All evaluations are run using only monocular camera data. The Central Management Interface is used to stream the dataset to the agents and my library *Multi-Agent EVO* is used to provide the Absolute Trajectory Error (ATE) metric, as defined by [43].

---

<sup>1</sup>My original extensions can be found in Appendix B

### 4.2.1 EuRoC Machine Hall

The EuRoC Machine Hall dataset [32] is one of the most widely used visual SLAM datasets, providing a 752x480 20fps video feed and millimeter-level ground truth data at 20hz. The camera rig is attached to a Micro Aerial Vehicle which flies through a machine room of approximately 15x15 meters in size. In line with other research, I simulate a multi-agent dataset by running the Machine Hall 01-03 scenarios in parallel on three agents.

Figure 4.1 presents the root mean square (RMS) absolute trajectory error and total data transfer of my distributed system running this dataset. **The median RMS ATE is 5.9cm over the 279-meter total trajectory length**, demonstrating my system’s very impressive accuracy. The 5 trials’ ATE have a 1.4cm spread around the median respectively, demonstrating the repeatability and robustness of my system.

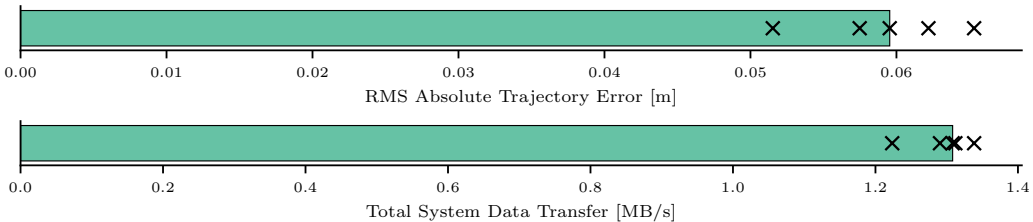


**Figure 4.1:** Plot the RMS absolute trajectory error and total data transfer rate of running the EuRoC Machine Hall 01-03 dataset 5 times on my system.

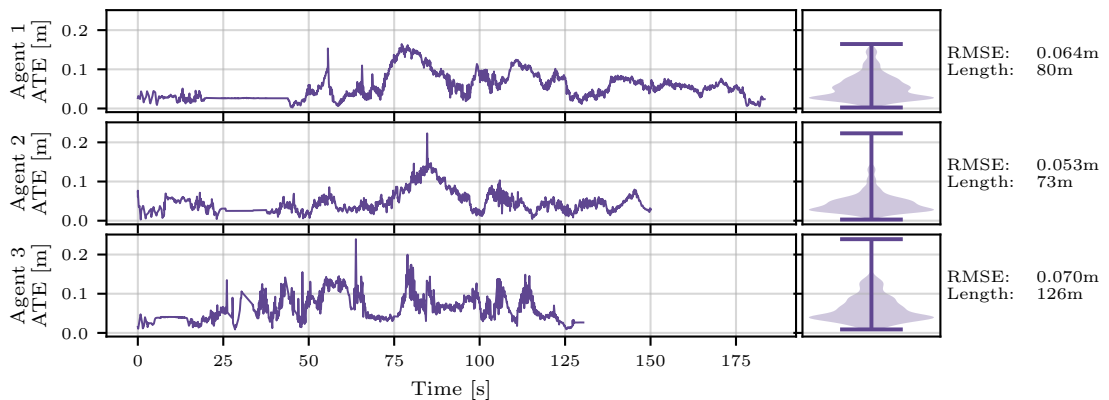


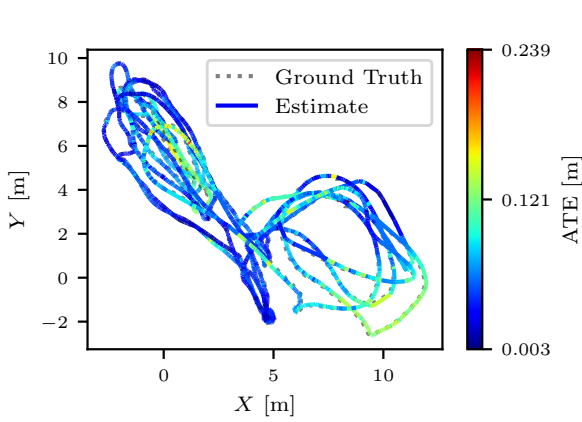
**Figure 4.2:** Plot of my system’s absolute trajectory error (ATE) with respect to the ground truth when running the EuRoC Machine Hall 01-03 scenarios in parallel on three agents.

To further analyze the characteristics of my SLAM system, we will focus on an individual trial. Figure 4.3 displays the full trajectory of the three agents compared to the ground truth, demonstrating my system’s high global accuracy and relative positioning. Figure 4.2 plots the ATE as the trial progresses. **It is clear that my system is performing SLAM as opposed to simple visual odometry** as the ATE returns to the baseline at the end of the trial when the agents return to their starting positions, with no accumulated drift.

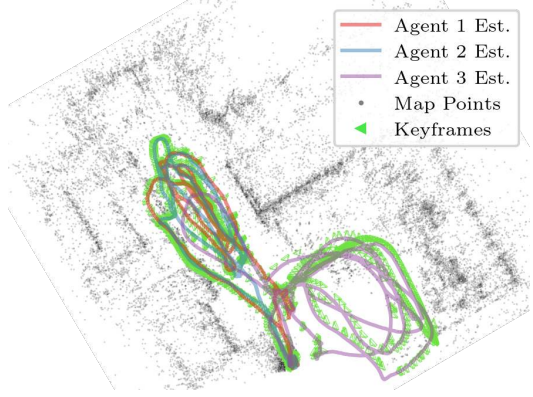
We now analyze the network usage presented in Figure 4.4. Initially, the agents send bag of word information before quickly detecting a merge opportunity. The agents exchange their maps, which can be seen in the large initial spike in network bandwidth. After a successful merge, they begin exchanging keyframes. The rate of keyframe data fluctuates depending on how much new area the agents are exploring.

Along with sending keyframes, the agents sporadically send map points to refine their map alignment. This occurs less frequently the longer system runs due to the additive increase multiplicative decrease method used to schedule map alignments, described in the Map Alignment

Refiner section. However, the size of the messages also grows over time due to the growing map.

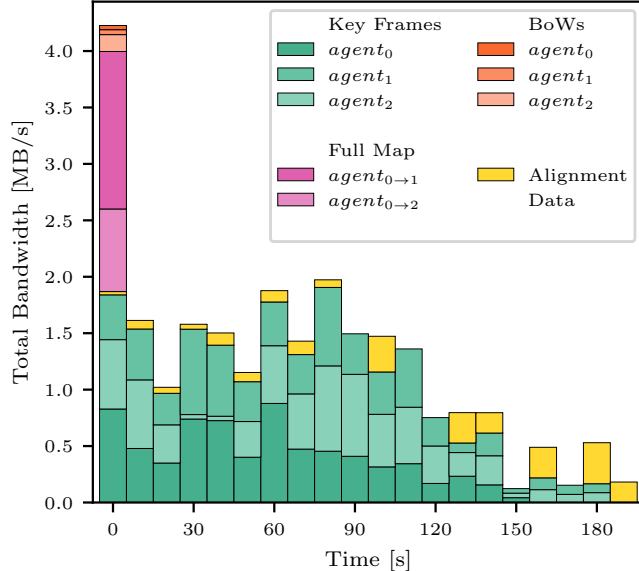


(a) Estimated trajectory and ground truth.



(b) Final map and individual agent trajectories.

**Figure 4.3:** EuRoC Machine Hall 01-03. A video recording of the trial gives a 3D visualization of the map and is available at 1m06s of the supplementary video<sup>1</sup>.



(a) Total system data over time, segregated by message type

	KB	Avg. KB/s
Key Frames	<i>agent</i> <sub>0</sub>	69,971
	<i>agent</i> <sub>1</sub>	63,908
	<i>agent</i> <sub>2</sub>	65,164
BoWs	<i>agent</i> <sub>0</sub>	371
	<i>agent</i> <sub>1</sub>	437
	<i>agent</i> <sub>2</sub>	1,496
Full Map	<i>agent</i> <sub>0→1</sub>	13,953
	<i>agent</i> <sub>0→2</sub>	7,319
Alignment Data	22,560	113.6
<b>Total Data</b>	<b>245,218</b>	<b>1,233.1</b>

(b) Total system data by message type

	Sent		Received	
	KB	Avg. KB/s	KB	Avg. KB/s
<i>agent</i> <sub>0</sub>	114,585	576.2	131,005	658.8
<i>agent</i> <sub>1</sub>	64,345	323.6	173,554	872.8
<i>agent</i> <sub>2</sub>	66,660	335.2	164,606	827.7

(c) Data by agent

**Figure 4.4:** Bandwidth used by the EuRoC Machine Hall 01-03 scenarios running on my SLAM system.

#### 4.2.2 TUM-VI Rooms

The TUM visual-inertial dataset [33] consists of handheld fisheye 512x512 video with ground truth data. As before, I only use monocular visual data and combine the Room 1-3 sessions to simulate a multi-agent dataset. The “room” environment is used for this evaluation, which is a 3x3 meter motion capture lab with plain flat walls and some posters hung up. There is less texture in this environment than the machine hall, making visual-only SLAM difficult. As seen in the full trajectory estimate given in Figure 4.6, parts of the room are revisited dozens of times by different agents, allowing us to evaluate our system’s ability to relocalize agents within previously mapped environments.

<sup>1</sup>Supplementary video URL: <https://cam-diss.s3.amazonaws.com/video.mp4>

Figure 4.5 shows that the RMS ATE is very tightly clustered around the median of 6.95cm, with one outlier caused by an agent in that trial having a slightly un-optimal map merge. The tight clustering is most likely due to the small environment with areas being revisited many times, allowing the shared map to converge on a very similar solution each time. The lower data transfer rate of 0.84 MB/s is also due to the small environment, resulting in the agents having to share less information.

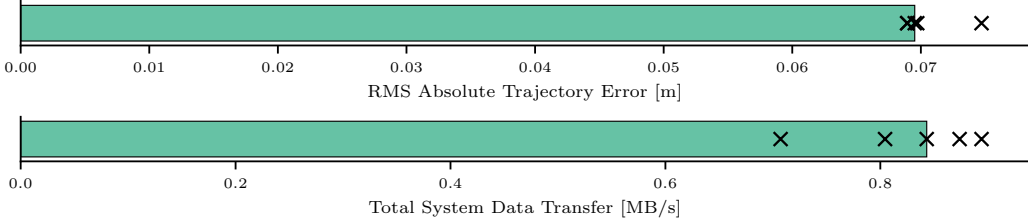


**Figure 4.5:** Plot the RMS ATE and Total Data Transfer rate of running the TUM-VI Rooms 1-3 dataset 5 times on my system.

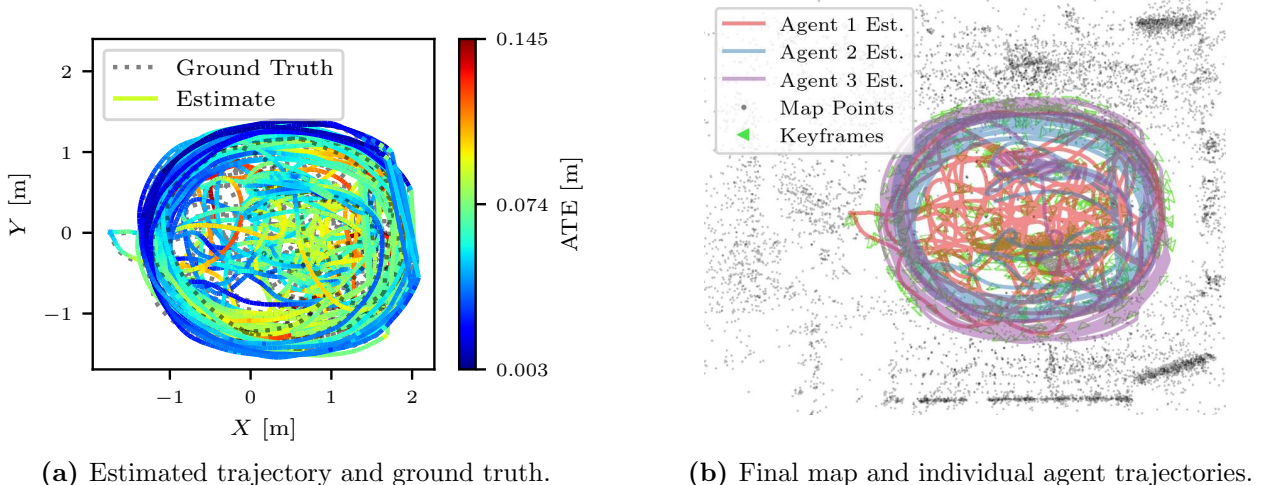


**Figure 4.6:** TUM-VI Rooms 01-03. A video recording of the trial gives a 3D visualization of the map and is available at 0m04s of the supplementary video<sup>1</sup>.

Once again, we focus on an individual trial to further evaluate my system. Figure 4.7 shows that there is **no long-term error built up**, demonstrating that my system is successfully localizing agents within the shared map and performing long-term map point association.

The data transfer characteristics are given by Figure A.1 in the appendix, and yield similar conclusions to that of the EuRoC Machine Hall dataset. The only difference to note is the smaller key frame and alignment data transfer rate due to the smaller environment.

### 4.3 Comparison to Related Work

As discussed in the Relevant Work section, to the best of my knowledge, my system is the only publically available decentralized monocular vision SLAM system. This makes direct comparisons with other multi-agent SLAM systems difficult, as they rely on more accurate but bulky sensors such as stereo cameras and LiDAR. However, this section still attempts to compare my system to the latest research in the field to give context on its performance relative to other state-of-the-art systems.

<sup>1</sup>Supplementary video URL: <https://cam-diss.s3.amazonaws.com/video.mp4>

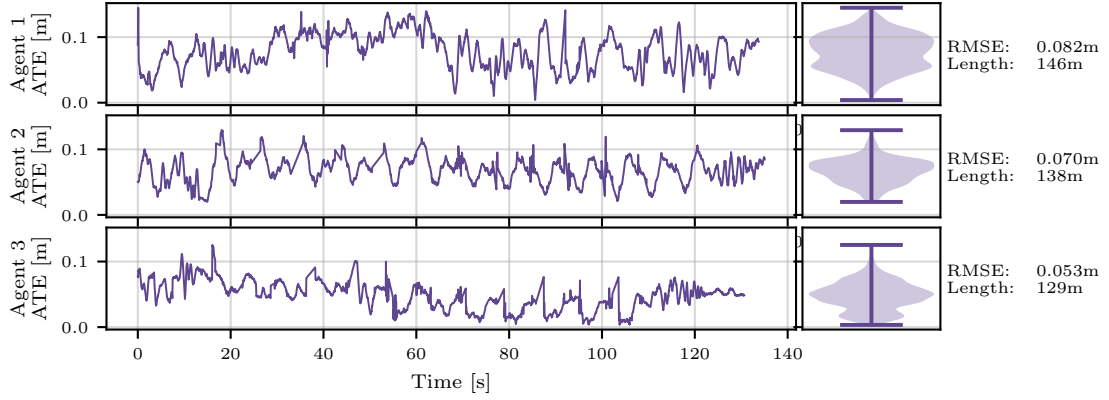


**Figure 4.7:** Plot of my system’s absolute trajectory error (ATE) with respect to the ground truth when running the TUM-VI Room 1-3 scenarios in parallel on three agents.

### 4.3.1 CCM-SLAM

Centralized Collaborative Monocular SLAM (CCM-SLAM) (2019) from the ETH Zurich Vision for Robotics Lab [15] is the most comparable multi-agent SLAM system in recent literature and is well-cited within the field. To my knowledge, it is the most recent monocular vision-capable multi-agent SLAM system.

It is important to note that CCM-SLAM is a *centralized* system, significantly simplifying their multi-agent SLAM problem compared to my distributed system. **Nevertheless, my system outperforms CCM-SLAM in terms of RMS absolute trajectory error, as presented in Figure 4.8.** Notably, CCM-SLAM failed all 5 trials of the TUM-VI Rooms dataset, due to its inability to relocalize an agent if localization is lost. This greatly reduces the robustness of their system as tracking is often lost in real-world use cases due to motion blur or a lack of visible features. The latter is the reason for CCM-SLAM’s failures on the TUM-VI dataset, as the environment contains plain walls which may cause a brief loss of tracking.

### 4.3.2 VINS-Mono Multisession SLAM

VINS-Mono (2018) [44] is a popular open-source *single-agent* monocular vision SLAM system with multisession capabilities. This allows multiple datasets to be played consecutively, with each session building upon the map built by the previous sessions. This is an easier problem than multi-agent SLAM, where the sessions are run in parallel and agents share their maps in real-time. In addition, VINS-Mono requires inertial data, so it is not a purely monocular vision system. **As presented in Figure 4.8, my system still outperforms VINS-Mono multisession.**

	My system	CCM-SLAM <sup>1</sup>	VINS-Mono <sup>2</sup>
EuRoC Machine Hall 01-03	<b>0.059</b>	0.077	0.074
Tum-VI Rooms 1-3	<b>0.070</b>	FAILED	0.256

**Figure 4.8:** RMS absolute trajectory error of my SLAM system relative to comparable state-of-the-art multi-agent systems. All results are taken as the median of 5 trials.

<sup>1</sup>CCM-SLAM is a centralized system, as opposed to my decentralized system.

<sup>2</sup>VINS-Mono is a single-agent SLAM system run in multisession mode. Additionally, it requires inertial data, unlike the other two systems.

The difference in performance is particularly pronounced in the TUM-VI Rooms dataset. This was due to their system only merging agents’ maps locally – once an agent moved away from

the merge site, it began creating an entirely new map instead of reusing the map built by the previous agent. Therefore, the global consistency of the shared map was lacking which resulted in the high RMS ATE of the combined trajectories.

### 4.3.3 Comparison to Single-Agent SLAM Systems

We would hypothesize that a multi-agent SLAM system will have higher accuracy than a comparable single-agent system, due to the increased available data. However, the reality is far more complex than this simple assumption. Figure 4.9 presents my multi-agent system’s errors compared to ORB-SLAM3 running the datasets individually. ORB-SLAM3 is widely regarded as the most accurate single-agent SLAM system currently available, so it is no surprise that it performs very well.

It can be observed that my system only has a marginal improvement in error over the single-agent system, which I hypothesize is the result of the varying ability among agents to utilize the shared map. For example, the TUM-VI Room environment is very small and areas of the map are revisited dozens of times in one session. This reduces the benefit of the increased data provided by a multi-agent system as a single session already observes more than enough data to build an accurate map of the world.

We see a significant improvement in error for the EuRoC Machine Hall 02 session, likely due to the 02 agent closely following the 01 agent. Conversely, the 01 session’s error is not reduced, likely because it leads the way for the 02 session. The 03 session explores a separate part of the environment from the other sessions, so a similar performance is to be expected.

	My system <sup>1</sup>	ORB-SLAM3 <sup>2</sup>
EuRoC MH 01	0.051	<b>0.049</b>
EuRoC MH 02	<b>0.048</b>	0.099
EuRoC MH 03	<b>0.058</b>	0.062
TUM-VI Room 1	0.072	<b>0.071</b>
TUM-VI Room 2	<b>0.048</b>	0.050
TUM-VI Room 3	<b>0.041</b>	0.042

**Figure 4.9:** Comparison of RMS ATE from my distributed SLAM system and the single-agent ORB-SLAM. All results are the median of 5 runs.

<sup>1</sup>Trajectories are aligned with the ground truth on a per-agent basis so we can compare each agent’s performance in isolation.

<sup>2</sup>Results are generated by running ORB-SLAM3 with its default settings for the EuRoC dataset.

On a broader note, many researchers believe single-agent SLAM to be a solved problem. This is reflected by the results seen here, where the single-agent system produces incredibly low trajectory errors that even multi-agent systems with far more data struggle to improve upon. We can not forget that these systems are already producing errors in the *centimeter* range for trajectories that are *hundreds of meters* long. This phenomenon is not something specific to my system – many other multi-agent systems do not have significantly higher accuracies than single-agent systems.

Therefore, I believe that the primary benefits of a multi-agent system are in its ability to provide relative positioning for path planning and collision avoidance, as well as building a shared map of the environment which is useful in applications such as search and rescue or cave mapping.

## 4.4 Real World Experiments

Deploying my system on physical robots demonstrates its ability to be run in real-time within the computational, bandwidth, and latency constraints of real-world systems. Furthermore, it demonstrates the robustness of my development framework which allowed seamless migration from local testing using simulations to a real distributed system using live camera feeds with no changes to my code base.

#### 4.4.1 Multi-Agent Collision Avoidance

In this experiment, I showcase collision avoidance between two robots. Real-time relative position data from the SLAM system is fed to the NMPC collision avoidance motion controller which controls the robot's velocity to avoid collisions. The SLAM system is running locally on each Cambridge RoboMaster, with communication facilitated by a router in the lab.

Figure 4.10 tests the system in an intersection environment, where the two robots would normally collide. The agents are able to localize each other **even when their views do not overlap and they can not see each other**, demonstrating that a shared map is being built by my SLAM system. **This would not be possible with traditional LiDAR collision avoidance or vision-based machine learning systems.**

Out of the four consecutive trials run in this environment, there were zero collisions between the two agents, and Figure 4.11 shows that the distance between agents never went below the collision threshold of 0.55 meters. Figure 4.12 shows the absolute trajectory error of the 4 trials, with an RMS ATE of only 7.4cm over the 50-meter-long trajectory.

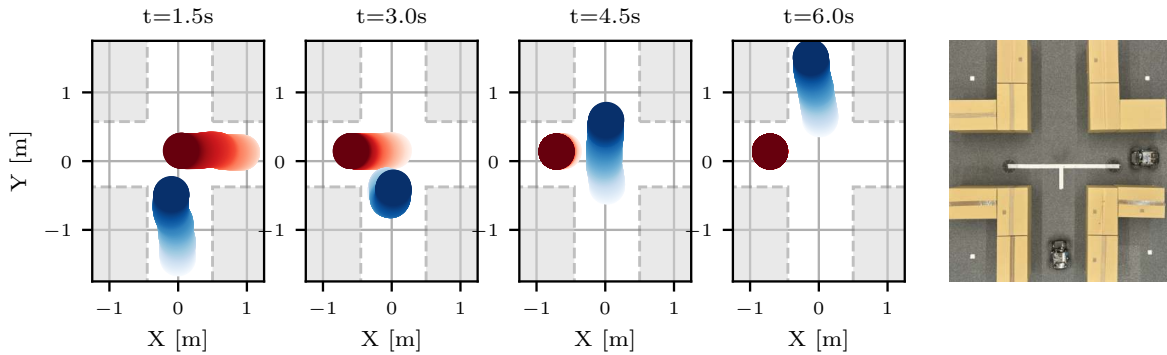


**Figure 4.10:** Demonstration of multi-agent collision avoidance. Two robots are set 90° to each other in an intersection environment, with no direct view of the other robot and little visual overlap (right). The blue agent is given a goal pose on the other side of the intersection and successfully avoids a collision when the red agent is pushed through the intersection. The trajectories generated by the SLAM system are presented on the left charts.

For visual reference, a video recording of the trials is available at 1m26s of the supplementary video<sup>1</sup>.

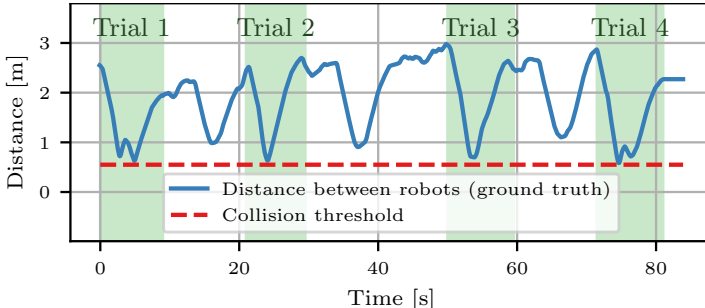


**Figure 4.11:** Plot of distance between the two robots throughout all four collision avoidance trials. The dips between trials are the robots' positions being reset.

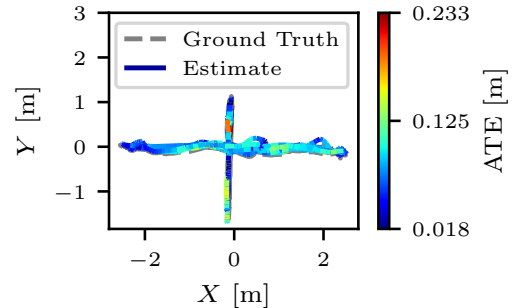


**Figure 4.12:** Collision avoidance estimated trajectory and ground truth. The RMS abs. trajectory error is 0.074 meters.

<sup>1</sup>Supplementary video URL: <https://cam-diss.s3.amazonaws.com/video.mp4>

# Chapter 5

## Conclusions

This project has exceeded my original success criteria: I have created a novel distributed visual SLAM system that performs better than comparable state-of-the-art systems and demonstrated real-world performance by deploying it on to physical robots. This is facilitated by a unique approach to the distributed pose graph estimation problem and the addition of features such as relocalization and long-term map reassocation.

In addition, I have developed a full suite of infrastructure including visualization, simulation, and evaluation tools, largely due to a lack of existing libraries for the relatively new field of multi-agent SLAM. All these tools, along with my core system, are made open-source with compiled Docker containers also provided.

### 5.1 Future Work

**Real-world deployment of multi-agent research.** Many interesting systems have been presented in the field of multi-agent robotics, such as reinforcement learning based path planning [45], and using collaborative aerial platforms for 3D printing [46] and bridge construction [47]. These systems have all been demonstrated in motion capture labs, however decentralized SLAM systems such as mine present a pathway towards their full-scale deployment in practical settings.

**Deep neural network feature extraction and matching.** In recent years there has been an exciting emergence of neural network based feature descriptors. SuperPoint [48] is an example of such a descriptor, providing impressively robust results. In addition, feature matchers such as LightGlue [49] are able to learn the geometric regularities of camera transformations through an end-to-end neural network training process to robustly match features across images, removing the need for the traditional RANSAC + epipolar geometry feature matching described in the Visual Odometry section. Leveraging such technologies in a multi-agent SLAM system may yield improved accuracy and robustness, especially in dynamic environments.

**Bandwidth optimization.** Ad-hoc mesh networks are necessary for the real-world deployment of distributed systems, however, their network capacity is often limited and some systems prefer broadcast messages over peer-to-peer. It is worth exploring how the data transfer characteristics of my system can be improved to better suit such a networking environment.

### 5.2 Lessons Learned

The most important lesson learned from this project is that cutting-edge research does not necessarily equate to well-written or documented code. I chose to use the single-agent ORB-SLAM3 system as the foundation of my project due to it being well-cited and widely regarded as the most accurate system available.

However, I quickly discovered that it was extremely hard to build upon their codebase. Large chunks of code were commented out without explanation, dataflow was hard to decipher, and it ran across four threads with poor concurrency control. Due to the above complexities, as well as it being my first time using C++, it took almost a month to get ORB-SLAM running, and many more before I began making good progress on the distributed aspect of the project – far longer than I had expected. In summary, I should have chosen a system based on the code quality and support from the researchers, as opposed to purely its performance.

# Bibliography

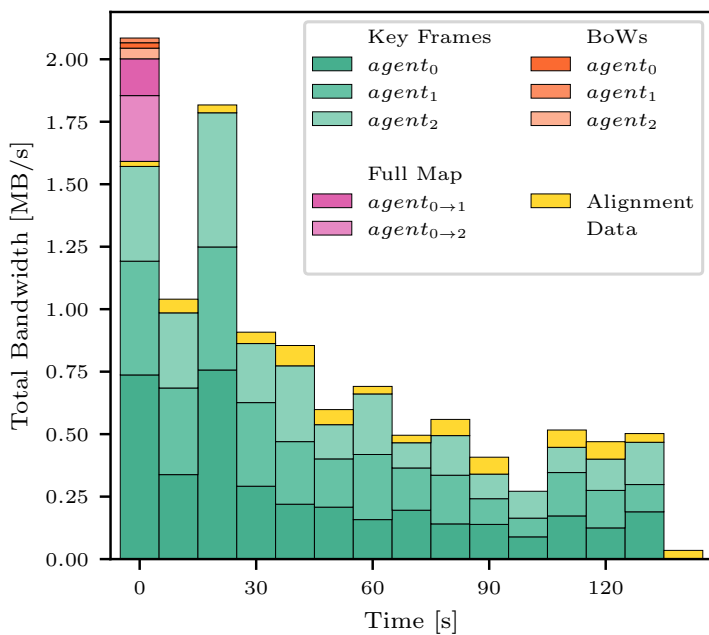
- [1] *ARCore*. <https://developers.google.com/ar/develop/fundamentals>.
- [2] *GraphNav*. <https://support.bostondynamics.com/s/article/GraphNav-Technical-Summary>.
- [3] Danping Zou, Ping Tan, and Wenzian Yu. “Collaborative visual SLAM for multiple agents: A brief survey”. In: *Virtual Reality & Intelligent Hardware* 1.5 (2019), pp. 461–482.
- [4] Jan Blumenkamp et al. *The Cambridge RoboMaster: An Agile Multi-Robot Research Platform*. Please note: the candidate’s name is stated in this paper. 2024. arXiv: 2405.02198 [cs.RO].
- [5] Carlos Campos et al. “ORB-SLAM3: An Accurate Open-Source Library for Visual, Visual-Inertial and Multi-Map SLAM”. In: *IEEE Transactions on Robotics* 37.6 (2021), pp. 1874–1890.
- [6] Dinar Sharafutdinov et al. “Comparison of modern open-source visual SLAM approaches”. In: *CoRR* abs/2108.01654 (2021). arXiv: 2108.01654. URL: <https://arxiv.org/abs/2108.01654>.
- [7] Xiang Gao and Tao Zhang. *Introduction to visual SLAM: from theory to practice*. Springer Nature, 2021.
- [8] Xiang Gao et al. *14 Lectures on Visual SLAM: From Theory to Practice*. Publishing House of Electronics Industry, 2017.
- [9] Hugh Durrant-Whyte and Tim Bailey. “Simultaneous localization and mapping: part I”. In: *IEEE robotics & automation magazine* 13.2 (2006), pp. 99–110.
- [10] Takafumi Taketomi, Hideaki Uchiyama, and Sei Ikeda. “Visual SLAM algorithms: A survey from 2010 to 2016”. In: *IPSJ transactions on computer vision and applications* 9 (2017), pp. 1–11.
- [11] Khalid Yousif, Alireza Bab-Hadiashar, and Reza Hoseinnezhad. “An Overview to Visual Odometry and Visual SLAM: Applications to Mobile Robotics”. In: *Intelligent Industrial Systems* 1 (Nov. 2015). DOI: 10.1007/s40903-015-0032-7.
- [12] Andreas Geiger et al. “Vision meets Robotics: The KITTI Dataset”. In: *International Journal of Robotics Research (IJRR)* (2013).
- [13] Ethan Rublee et al. “ORB: An efficient alternative to SIFT or SURF”. In: *2011 International Conference on Computer Vision*. 2011, pp. 2564–2571. DOI: 10.1109/ICCV.2011.6126544.
- [14] R. I. Hartley and A. Zisserman. *Multiple View Geometry in Computer Vision*. Second. Cambridge University Press, ISBN: 0521540518, 2004.
- [15] Patrik Schmuck and Margarita Chli. “CCM-SLAM: Robust and efficient centralized collaborative monocular simultaneous localization and mapping for robotic teams”. In: *Journal of Field Robotics* 36.4 (2019), pp. 763–781.
- [16] Patrik Schmuck et al. “Covins: Visual-inertial slam for centralized collaboration”. In: *2021 IEEE International Symposium on Mixed and Augmented Reality Adjunct (ISMAR-Adjunct)*. IEEE. 2021, pp. 171–176.

- [17] Xin Zhou et al. “Swarm of micro flying robots in the wild”. In: *Science Robotics* 7.66 (2022), eabm5954. DOI: 10.1126/scirobotics.abm5954. eprint: <https://www.science.org/doi/pdf/10.1126/scirobotics.abm5954>. URL: <https://www.science.org/doi/abs/10.1126/scirobotics.abm5954>.
- [18] Suvam Patra et al. “EGO-SLAM: A Robust Monocular SLAM for Egocentric Videos”. In: *2019 IEEE Winter Conference on Applications of Computer Vision (WACV)*. 2019, pp. 31–40. DOI: 10.1109/WACV.2019.00011.
- [19] Pengxiang Zhu et al. “Distributed Visual-Inertial Cooperative Localization”. In: *CoRR* abs/2103.12770 (2021). arXiv: 2103.12770. URL: <https://arxiv.org/abs/2103.12770>.
- [20] Ruwan Egodagamage and Mihran Tuceryan. “A collaborative Augmented Reality framework based on Distributed Visual SLAM”. In: *2017 International Conference on Cyber-worlds (CW)*. IEEE. 2017, pp. 25–32.
- [21] Xieyuanli Chen et al. “Distributed monocular multi-robot slam”. In: *2018 IEEE 8th annual international conference on CYBER technology in automation, control, and intelligent systems (CYBER)*. IEEE. 2018, pp. 73–78.
- [22] Guillaume Bresson, Romuald Aufrère, and Roland Chapuis. “Real-time decentralized monocular slam”. In: *2012 12th International Conference on Control Automation Robotics & Vision (ICARCV)*. IEEE. 2012, pp. 1018–1023.
- [23] Hao Xu et al. “ $D^2$ SLAM: Decentralized and Distributed Collaborative Visual-inertial SLAM System for Aerial Swarm”. In: *arXiv preprint arXiv:2211.01538* (2022).
- [24] Yulun Tian et al. “Kimera-Multi: Robust, Distributed, Dense Metric-Semantic SLAM for Multi-Robot Systems”. In: *IEEE Transactions on Robotics* 38.4 (2022), pp. 2022–2038. DOI: 10.1109/TR.2021.3137751.
- [25] Pierre-Yves Lajoie and Giovanni Beltrame. “Swarm-SLAM: Sparse Decentralized Collaborative Simultaneous Localization and Mapping Framework for Multi-Robot Systems”. In: *IEEE Robotics and Automation Letters* 9.1 (2024), pp. 475–482. DOI: 10.1109/LRA.2023.3333742.
- [26] P. Lajoie et al. “DOOR-SLAM: Distributed, Online, and Outlier Resilient SLAM for Robotic Teams”. In: *IEEE Robotics and Automation Letters* 5.2 (2020), pp. 1656–1663.
- [27] Pierre-Yves Lajoie and Giovanni Beltrame. “Swarm-SLAM: Sparse Decentralized Collaborative Simultaneous Localization and Mapping Framework for Multi-Robot Systems”. In: *IEEE Robotics and Automation Letters* 9.1 (Jan. 2024), pp. 475–482. ISSN: 2377-3774. DOI: 10.1109/lra.2023.3333742. URL: <http://dx.doi.org/10.1109/LRA.2023.3333742>.
- [28] Zhimin Peng et al. “ARock: An Algorithmic Framework for Asynchronous Parallel Coordinate Updates”. In: *SIAM Journal on Scientific Computing* 38.5 (Jan. 2016), A2851–A2879. ISSN: 1095-7197. DOI: 10.1137/15m1024950. URL: <http://dx.doi.org/10.1137/15M1024950>.
- [29] Siddharth Choudhary et al. “Distributed Mapping with Privacy and Communication Constraints: Lightweight Algorithms and Object-based Models”. In: *CoRR* abs/1702.03435 (2017). arXiv: 1702.03435. URL: <http://arxiv.org/abs/1702.03435>.
- [30] B. W. Boehm. “A spiral model of software development and enhancement”. In: *Computer* 21.5 (1988), pp. 61–72. DOI: 10.1109/2.59.
- [31] O. Michel. “Webots: Professional Mobile Robot Simulation”. In: *Journal of Advanced Robotics Systems* 1.1 (2004), pp. 39–42. URL: <http://www.ars-journal.com/International-Journal-of-%20Advanced-Robotic-Systems/Volume-1/39-42.pdf>.

- [32] Michael Burri et al. “The EuRoC micro aerial vehicle datasets”. In: *The International Journal of Robotics Research* 35.10 (2016), pp. 1157–1163.
- [33] David Schubert et al. “The TUM VI Benchmark for Evaluating Visual-Inertial Odometry”. In: *2018 IEEE/RSJ International Conference on Intelligent Robots and Systems (IROS)*. 2018, pp. 1680–1687. DOI: 10.1109/IROS.2018.8593419.
- [34] *GNU General Public License*. <http://www.gnu.org/licenses/gpl.html>. Version 3. Free Software Foundation, June 29, 2007.
- [35] *The MIT License*. <https://opensource.org/license/mit>.
- [36] *Boost C++ Libraries*. <https://www.boost.org/>.
- [37] Dorian Gálvez-López and J. D. Tardós. “Bags of Binary Words for Fast Place Recognition in Image Sequences”. In: *IEEE Transactions on Robotics* 28.5 (Oct. 2012), pp. 1188–1197. ISSN: 1552-3098. DOI: 10.1109/TRO.2012.2197158.
- [38] Hyeong Ryeol Kam et al. “RViz: a toolkit for real domain data visualization”. In: *Telecommunications Syst.* 60.2 (Oct. 2015), pp. 337–345. ISSN: 1018-4864. DOI: 10.1007/s11235-015-0034-5. URL: <https://doi.org/10.1007/s11235-015-0034-5>.
- [39] *Foxglove Studio*. <https://foxglove.dev/>.
- [40] Mina Kamel et al. “Nonlinear Model Predictive Control for Multi-Micro Aerial Vehicle Robust Collision Avoidance”. In: *CoRR* abs/1703.01164 (2017). arXiv: 1703.01164. URL: <http://arxiv.org/abs/1703.01164>.
- [41] Michael Grupp. *evo: Python package for the evaluation of odometry and SLAM*. <https://github.com/MichaelGrupp/evo>. 2017.
- [42] *OptiTrack for Robotics*. <https://optitrack.com/applications/robotics/>. Accessed: 2024-04-05.
- [43] Jürgen Sturm et al. “A benchmark for the evaluation of RGB-D SLAM systems”. In: *2012 IEEE/RSJ International Conference on Intelligent Robots and Systems*. 2012, pp. 573–580. DOI: 10.1109/IROS.2012.6385773.
- [44] Tong Qin, Peiliang Li, and Shaojie Shen. “VINS-Mono: A Robust and Versatile Monocular Visual-Inertial State Estimator”. In: *IEEE Transactions on Robotics* 34.4 (2018), pp. 1004–1020. DOI: 10.1109/TRO.2018.2853729.
- [45] Matteo Bettini et al. “VMAS: a vectorized multi-agent simulator for collective robot learning”. In: *International Symposium on Distributed Autonomous Robotic Systems*. Springer. 2022, pp. 42–56.
- [46] Ketao Zhang et al. “Aerial additive manufacturing with multiple autonomous robots”. In: *Nature* 609.7928 (2022), pp. 709–717.
- [47] AMMAR MIRJAN et al. “BUILDING WITH FLYING ROBOTS”. In: *Fabricate 2014: Negotiating Design & Making*. DGO - Digital original. UCL Press, 2017, pp. 266–271. URL: <http://www.jstor.org/stable/j.ctt1tp3c5w.36> (visited on 05/07/2024).
- [48] Daniel DeTone, Tomasz Malisiewicz, and Andrew Rabinovich. “SuperPoint: Self-Supervised Interest Point Detection and Description”. In: *CVPR Deep Learning for Visual SLAM Workshop*. 2018. URL: <http://arxiv.org/abs/1712.07629>.
- [49] Philipp Lindenberger, Paul-Edouard Sarlin, and Marc Pollefeys. *LightGlue: Local Feature Matching at Light Speed*. 2023. arXiv: 2306.13643 [cs.CV].

# Appendix A

## Additional Figures



(a) Total system data over time, segregated by message type

		KB	Avg. KB/s
Key Frames	$agent_0$	37,599	264.9
	$agent_1$	33,066	233.0
	$agent_2$	29,963	211.1
BoWs	$agent_0$	217	1.5
	$agent_1$	188	1.3
	$agent_2$	426	3.0
Full Map	$agent_{0 \rightarrow 1}$	1,472	10.4
	$agent_{0 \rightarrow 2}$	2,631	18.5
Alignment Data		6,947	49.0
<b>Total Data</b>		<b>112,511</b>	<b>792.8</b>

(b) Total system data by message type

	Sent		Received	
	KB	Avg. KB/s	KB	Avg. KB/s
$agent_0$	<b>49,083</b>	<b>345.9</b>	<b>63,644</b>	<b>448.5</b>
$agent_1$	<b>33,254</b>	<b>234.3</b>	<b>76,624</b>	<b>539.9</b>
$agent_2$	<b>30,389</b>	<b>214.1</b>	<b>80,649</b>	<b>568.3</b>

(c) Data by agent

**Figure A.1:** Bandwidth used by the TUM-VI Rooms 01-03 scenarios running on my SLAM system.

# **Appendix B**

## **Project Proposal**

# 1 Introduction

Visual simultaneous localization and mapping (Visual SLAM) is a technology used to localize the 6dof pose of a camera sensor while also creating a 3D map of the captured environment. Visual SLAM is often used in systems such as self-driving cars, augmented reality devices, and autonomous drones due to the low cost and weight of camera sensors when compared to the sensors used in other SLAM systems such LIDAR, RGB-D cameras or Radar.

While there have been many advanced implementations of visual SLAM over the last decade, very few of them have focused on distributed multi-agent systems, instead focusing on single-agent (e.g. ORB-SLAM3 [1]) or centralized multi-agent systems (e.g. CCM-SLAM [2]). Distributed multi-agent visual SLAM systems have broad reaching use cases, as the lack of a centralized management server allows the system to be robust to failure and used in environments where network infrastructure may be lacking, such as autonomous drone swarms in search and rescue operations or collaboration amongst self-driving cars.

My project aims to implement a distributed multi-agent visual SLAM system, where agents are able to share information with each other to enable more accurate localization and collaboration in map building.

Key components of this project include:

1. Create an environment for testing and evaluating a multi-agent visual SLAM system locally.
2. Designing and implement a communication layer to enable agents to serialize/deserialize key datastructures (e.g. Keyframes, Map Points, etc.) and share information with each other.
3. Ensure robust performance, even when connectivity between agents is degraded.

Possible extensions to this project include:

1. Enable agents to intelligently share information to their peers, only sending map fragments that are relevant.
2. Distributing calculations amongst the different agents, preventing the duplication of computationally intensive work such as global bundle adjustment. One possible approach would be to leverage gaussian belief propagation, a message passing algorithm to optimize a factor graph representation of the bundle adjustment problem.
3. Map compression algorithms.
4. Adding additional sensors such as ultra-wideband sensors to better localize drones using sensor fusion.

## 2 Starting Point

Visual SLAM systems are a mature and well researched subfield of Computer Science, with many advanced implementations. To avoid spending the majority of my time re-implementing a visual SLAM system, I will instead be using an existing **single-agent** visual SLAM implementation as a starting point for my project. This will allow me to focus my efforts on the distributed aspect of my project, which I believe is novel and under-researched in the field. Furthermore, by using a cutting edge single-agent SLAM system as a foundation for my project, I hope to be able to create a distributed SLAM system that is accurate and performant enough to have real-world use cases.

Thus far, I have forked the ORB-SLAM3 git repository<sup>12</sup> [1] and made minor changes to the codebase to allow it to run on my machine.

I have no prior experience working with SLAM systems, but I have done research on the current state of multi-agent visual SLAM systems to evaluate the feasibility of my project, and to try prevent it being a duplication of past work.

## 3 Evaluation

I will evaluate this project by comparing my multi-agent system to a comparable single-agent system when run on the same dataset. This will involve:

- Quantitatively comparing the RMS error of the predicted trajectory to the ground truth.
- Qualitatively comparing the maps generated by both systems, particularly how much area they cover.

Additionally, I will evaluate any extensions (if applicable) as follows:

- Extension 1 & 3: Reduction to total bytes sent between nodes in the system.
- Extension 2: Reduction in total computation done by multi-agent system.
- Extension 4: Improvement in localization performance.

To evaluate my system, I plan on using a combination of popular public datasets (e.g. EuRoC [3], KITTI [4]) self-made datasets and datasets generated in the Cambridge Multi-Robot and Multi-Agent Systems Lab<sup>3</sup>.

---

<sup>1</sup>ORB-SLAM3 is a cutting edge visual SLAM implementation published in 2021 by Campos et al.

<sup>2</sup>[https://github.com/UZ-SLAMLab/ORB\\_SLAM3](https://github.com/UZ-SLAMLab/ORB_SLAM3)

<sup>3</sup><https://proroklab.org>

## 4 Success Criteria

For the project to be deemed a success, the following must be successfully completed:

1. Create an implementation of a multi-agent visual SLAM system, with the following capabilities:
  - (a) Multiple agents will be able to localize themselves within a world using purely visual data.
  - (b) Agents will be capable of communicating with each other to build a shared understanding of the world.
  - (c) Agents will be able to act independently, failing gracefully if it loses communication with its peers.
2. Evaluate the capabilities of the system, following the guidelines set out in section 3

## 5 Timetable and Milestones

### Weeks 1 to 2 (16 October - 29 October)

Get single-agent open source visual SLAM implementations running from the research code provided. Explore possible simulators and integrate them with the visual SLAM program.

### Weeks 3 to 4 (30 October - 12 November)

Continue preparatory work and set up a solid development environment for me to use when writing my own code. Includes figuring out how to develop and run a distributed system on my local machine.

### Weeks 5 to 6 (13 November - 26 November)

Create/find a dataset to test my distributed visual SLAM implementation on.

Begin implementing distributed visual SLAM, with the different instances communicating with each other and sharing information.

### Weeks 7 to 8 (27 November - 10 December)

Continue implementing distributed visual SLAM system.

### Weeks 9 to 11 (11 December - 31 December)

Holiday & revision.

### Weeks 12 to 13 (1 January - 14 January)

Holiday & revision.

Continue implementing distributed visual SLAM system.

### Weeks 14 to 15 (15 January - 28 January)

Explore implementing extension 1 to intelligently share information with peers, only sending over useful parts of the map to them.

## **Weeks 16 to 17 (29 January - 11 February)**

Continue implementing distributed visual SLAM system and extension 1.

Spend time on other additional goals if I have time.

## **Weeks 18 to 19 (12 February - 25 February)**

Explore implementing extension 2 to prevent the duplication of work spent on doing global bundle adjustments.

## **Weeks 20 to 21 (26 February - 10 March)**

Begin evaluating project and writing dissertation.

## **Weeks 22 to 23 (11 March - 24 March)**

Continue evaluating project and writing dissertation.

## **Weeks 24 to 25 (25 March - 7 April)**

Submit draft of dissertation to supervisor and DOS and make improvements.

Set aside time for exam revision.

## **Weeks 26 to 27 (8 April - 21 April)**

Finalize dissertation and get any final feedback.

Set aside time for exam revision.

## **Weeks 28 - 29 (22 April - 5 May)**

Padding for any final work to be done.

Set aside time for exam revision.

## **Week 30 (10 May)**

Dissertation Deadline

## 6 Resource Declaration

I will be using my personal laptop (MacBook Air M2) as my primary machine for software development, along with Git to continuously back up my code and dissertation to the cloud in the event of any hardware failure. *I accept full responsibility for this machine and I have made contingency plans to protect myself against hardware and/or software failure.*

I have asked for permission to use the Robotics Lab whenever it is free, as it does not have a booking system. This is not a critical resource, as I have multiple dataset sources as noted in section 3.

## References

- [1] Carlos Campos et al. “ORB-SLAM3: An Accurate Open-Source Library for Visual, Visual-Inertial and Multi-Map SLAM”. In: *IEEE Transactions on Robotics* 37.6 (2021), pp. 1874–1890.
- [2] Patrik Schmuck and Margarita Chli. “CCM-SLAM: Robust and efficient centralized collaborative monocular simultaneous localization and mapping for robotic teams”. In: *Journal of Field Robotics* 36.4 (2019), pp. 763–781.
- [3] Michael Burri et al. “The EuRoC micro aerial vehicle datasets”. In: *The International Journal of Robotics Research* 35.10 (2016), pp. 1157–1163. DOI: 10 . 1177 / 0278364915620033. eprint: <https://doi.org/10.1177/0278364915620033>. URL: <https://doi.org/10.1177/0278364915620033>.
- [4] A Geiger et al. “Vision meets robotics: The KITTI dataset”. In: *The International Journal of Robotics Research* 32.11 (2013), pp. 1231–1237. DOI: 10 . 1177 / 0278364913491297. eprint: <https://doi.org/10.1177/0278364913491297>. URL: <https://doi.org/10.1177/0278364913491297>.